

Rheology discussions: The physics of dense suspensions

Safa Jamali, Emanuela Del Gado, and Jeffrey F. Morris

Citation: *Journal of Rheology* **64**, 1501 (2020); doi: 10.1122/8.0000174

View online: <https://doi.org/10.1122/8.0000174>

View Table of Contents: <https://sor.scitation.org/toc/jor/64/6>

Published by the [The Society of Rheology](#)

ARTICLES YOU MAY BE INTERESTED IN

[Preface: Physics of dense suspensions](#)

Journal of Rheology **64**, 223 (2020); <https://doi.org/10.1122/8.0000016>

[A constitutive model for simple shear of dense frictional suspensions](#)

Journal of Rheology **62**, 457 (2018); <https://doi.org/10.1122/1.4999237>

[A constitutive model for sheared dense suspensions of rough particles](#)

Journal of Rheology **64**, 1107 (2020); <https://doi.org/10.1122/8.0000039>

[Shear thickening, frictionless and frictional rheologies in non-Brownian suspensions](#)

Journal of Rheology **58**, 1693 (2014); <https://doi.org/10.1122/1.4890747>

[Shear thickening in dense non-Brownian suspensions: Viscous to inertial transition](#)

Journal of Rheology **64**, 227 (2020); <https://doi.org/10.1122/1.5129680>

[A review of thixotropy and its rheological modeling](#)

Journal of Rheology **63**, 477 (2019); <https://doi.org/10.1122/1.5055031>



DISCOVER the **RHEOMETER** with the...
Sensitivity • Ease-of-use • Versatility
to address the most **demanding** applications

The **NEW Discovery Hybrid Rheometer**





Rheology discussions: The physics of dense suspensions

Safa Jamali,¹ Emanuela Del Gado,² and Jeffrey F. Morris³

¹*Department of Mechanical and Industrial Engineering, Northeastern University, Boston, Massachusetts 02115*

²*Department of Physics and Institute for Soft Matter Synthesis and Metrology, Georgetown University, Washington, DC 20057*

³*Bejamin Levich Institute and Department of Chemical Engineering, CUNY City College of New York, New York, New York 10031*

(Received 18 October 2020; published 16 November 2020)

The following set of discussions is a complement to the recent special issue of the *Journal of Rheology* on the Physics of Dense Suspensions edited by two of us [1]. The discussions took place during the virtual symposium entitled “Physics of Dense Suspensions” (PDS) held on July 9–10, 2020, in response to the broad interest raised by the special issue. Soon after the special issue appearance, in fact, the COVID-19 pandemic resulted in the loss of standard in-person meeting venues. A virtual meeting was, organized to accommodate the desire expressed by many to discuss the fundamental questions brought to focus. The symposium, which was free of charge, attracted more than 500 registered participants from around the world and provided a platform for presentations by authors, followed by question-and-answer periods. The latter periods were characterized by quite lively discussions, out of which grew some consensus but also some points of vigorous debate. The following set of questions and answers by the symposium participants summarizes those discussions and we hope will promote continued development of research ideas in this area of rheology.

The questions and answers collected here concern 22 papers from the *Journal of Rheology* special issue, along with a number of other papers published in other journals on the most recent developments in the study of suspensions, from theoretical, computational, and experimental perspectives.

While the debate on a number of aspects of the physics of dense suspension remains open, a consensus has emerged over the past few years on the micromechanical description of the shear-thickening phenomenon: as the particle motion becomes hindered, increasingly larger stresses are exhibited in response to an applied deformation rate. However, hindrance in different modes of motion—translation, rotation, and twisting—is impacted at the particle scale by *microscopic interactions*. These interactions, which may occur at nanometer scale in the “contact” zones between particles, together with the imposed flow result in force chains, clusters, and networks that may even span the entire suspension. Characterizing these force networks, their fluctuations, and relaxations in a *statistical mechanics framework* holds the key to stress propagation and response

throughout the suspension. The microscopic interactions and their statistical description are the essential underpinnings of the rich rheological responses of dense suspensions to an applied deformation or stress. For broad utilization of the understanding, *constitutive models* are required to describe and predict the relationship between these microscopic mechanisms, the dynamical heterogeneities, normal stress differences, and ultimately the time- and rate-dependent rheology of dense suspensions. Ultimately, the real-world applications and systems of interest deviate from ideal cases where one mode of interaction or particle type and size can be studied in isolation. These *more complex systems*—where several modes of interactions are at play, soft or deformable particles are considered or other non-Newtonian behaviors are exhibited by the background fluid—benefit from the fundamental understanding developed in simpler models, but they simultaneously challenge that understanding and inform the next stage of research in the field.

Following the JOR special issue as a guideline, four distinct but closely related themes were identified as general discussion topics for the symposium, led by panels of rheologists representing a range of expertise. Thanks to the participation and the work of those experts, we could widen the scope of the discussion and branch out to the rheology community beyond the initial list of contributors. We list here the themes and discussion leaders, with additional thanks for the energy and useful direction of the interactions during the symposium.

Theme 1: Microscopic Interactions—measurements, models, and method development—Discussion leaders: John Brady, Jacinta Conrad, and Meera Ramaswamy;

Theme 2: Statistical Mechanics Framework—network formation and fluctuations—Discussion leaders: Heinrich Jaeger, Romain Mari, and Poornima Padmanabhan;

Theme 3: Constitutive Models—nonlinear models, hysteresis, and normal stress—Discussion leaders: Gareth McKinley, Peter Olmsted, and Rahul Chacko; and

Theme 4: More Complex System—geomorphology, soft particles, and viscoelastic suspensions—Discussion leaders: Chinedum Osuji, Itai Cohen, and Ruel McKenzie.

The papers presented and discussed within *Theme 1* [2–9] had as focus the different micromechanisms that can result in shear thickening of dense suspensions, and this was complemented by the description of experimental techniques and

Note: This paper is part of the special issue on Physics of Dense Suspensions.

protocols that have been devised to probe the microscopic interactions. Speakers in *Theme 2* presented a series of papers and unpublished works [10–16] focused on various statistical physics descriptions of microstructure evolution and microscopic fluctuations and properties under shear-thickening conditions. These papers covered both computational and experimental perspectives. *Theme 3* papers and unpublished work [17–23] addressed constitutive descriptions of dense suspensions in various conditions. These studies considered suspensions in extensional flow, upon impact, and undergoing shear flow, seeking to describe their nonlinear response, normal stresses, and heterogeneities. In *Theme 4*, studies describing a number of systems that deviate significantly from simpler model systems were presented, elucidating their complex and rich rheological behavior [24–31]. This theme outlined work from a series of papers on thixotropic particulate systems, geomorphological flows, suspensions of soft deformable particles, and complex granular systems.

Taken collectively, the papers on which the discussions are based seek understanding of the connections between different length scales—from microscopic origins of different forces to a continuum-level constitutive description of the entire suspension. The recent developments and the discussions during the symposium show that these efforts are intertwined in such a way that, while explorations may focus on one scale, a multiscale view is valuable. Looking to the future, more studies that help us to bridge the gap between the microscopic physics and tribology at the particle and smaller scales, particularly in the close interactions where contact modeling applies, to macroscopic rheology are needed; this set of investigations will involve mesoscale force networks and their evolution under flowing conditions. These investigations should include developments of both computational and experimental techniques to resolve details of contact interactions and particle motions. A point of consensus arising from the symposium was that there is a need to decouple and isolate the influence of different modes of surface interactions, perhaps guided by understanding from the field of tribology. The symposium clearly demonstrated, through the participant composition and the discussions developed, that substantive progress will require efforts to integrate understanding from statistical and granular physics, tribology, and rheology. The advances will, of course, impact our understanding of a wide range of natural phenomena, while helping us to guide the design of materials and processing conditions across a range of applications and industries, from geophysical flows to additive manufacturing and from slurries used in batteries to personal-care products.

In closing, we recognize AIP Publishing and the *Journal of Rheology* editors (Ralph Colby and Roseanna Zia) for their invaluable role in the recognition of the topic and for their constant support throughout the development of PDS special issue and symposium. We gratefully acknowledge all of our speakers and contributors, the discussion leaders, and all who are engaged in the conversations that followed. Finally, we would also like to recognize and thank Ali Shahmohammadi, Meera Ramaswamy, Edward Ong, Rishabh More, Mu Wang, and Joseph Barakat, who very

graciously did a great service to all of the community in forming a permanent record of the symposium by transcribing the verbal discussions and identifying the questions upon which the following written exchanges are based.

“Stress decomposition in LAOS of dense colloidal suspensions,” Edward Y. X. Ong, Meera Ramaswamy, Ran Niu, Neil Y. C. Lin, Abhishek Shetty, Roseanna N. Zia, Gareth H. McKinley, and Itai Cohen

Q1: You suggest that the Brownian stresses can be obtained after a certain equilibration time. Is the timescale for this equilibrium process always small enough so that you can be confident in the stress decomposition? (Peter Olmsted and Lilian Hsiao)

A1: We are interested in measuring the Brownian stress of the sheared suspension undergoing large amplitude oscillatory shear (LAOS), which is associated with the complex microstructure built up by the LAOS flow and particle interactions. This is different from the Brownian stress after the microstructure has equilibrated into a homogeneous state. Simulations predict that the initial stress decay immediately after shear cessation is very rapid and most of the Brownian stresses associated with packing decay within this short timescale. After this initial decay, the system equilibrates into a homogeneous state at a much slower rate (see, for example, [49] in our paper). Two properties are key for our measurement of the Brownian stresses: (i) The suspension microstructure is the same at a given point in the LAOS cycle over multiple cycles after the LAOS flow has achieved a steady state and (ii) the timescale of the stress decay in the cessation experiment is sufficiently long relative to our measurement timescales so that we can measure and extrapolate the Brownian stress data back to the point of cessation. We ensure the first is true by applying two full LAOS cycles prior to cessation or reversal and ensuring that the measurements are reproducible. For the second, it is difficult to calculate the exact relaxation time because it remains unclear which length scale is relevant for this relaxation behavior. It is also unclear how the diffusivity is enhanced as a result of the increased spatial and velocity correlation between particles due to particle packing effects, which is not considered in the Einstein diffusivity used conventionally. Nonetheless, we can still attempt to estimate this decay timescale. If we were to use the boundary layer $a/Pe \sim 10^{-10}$ m (where a is the radius of the particles and Pe is the Peclet number) as the relevant length scale and feed that into the calculation of the diffusion velocity, $v \sim D/a \sim 10^{-9}$ m/s, where $D \sim k_B T / 6\pi\eta a \sim 10^{-15}$ m²/s is the Einstein diffusivity, we obtain a minimum timescale $\tau \sim (a/Pe)v \sim 10^{-1}$ s, which agrees with the timescales obtained from our fits. The instrument inertia adjustment time is $\sim 10^{-1}$ s, and the sampling rate is 250 Hz, which allows us to capture the tail end of the decay activity. It will be worthwhile to probe the Brownian behavior in the dense limit as understanding of Brownian stress has been limited to mostly uniform microstructures at small Pe . The timescale measured from our experiment suggests that it is possible to use 3D image acquisition to capture the evolution of the microstructure during cessation. The main challenge for such an experiment is in building a shear cell that can set the shear rate to zero rapidly without introducing

additional artifacts to the measurement. Alternatively, 2D imaging of a dense 3D or quasi-2D suspension undergoing shear cessation on a rheometer may help to elucidate this issue. Simulations on shear cessation, which include Brownian, hydrodynamic, and contact stresses, will also be very helpful to provide some intuition on the problem.

Q2: *In our (Koumakis et al., PRL, 2013) [1] experimental and Brownian dynamics studies of hard-sphere glasses in LAOS, we observed similar memory effects as you have discussed at high frequencies, due to unrelaxed structural anisotropies at the maximum strain. Upon strain reversal, the system exhibits reduced stress until the structure becomes isotropic again. At low frequencies, however, those anisotropies are relaxed at the maximum strain and thus no “memory” is observed. Have you studied the intermediate range of frequencies? (George Petekidis)*

A2: The relaxation behavior for high Pe_ω described in Koumakis et al. [32] is similar to both our observation and interpretation of the Brownian stress right after the LAOS flow changes direction. As the focus of our paper was on demonstrating the stress decomposition experimental protocol, we did not probe the different ranges of frequencies as done in your paper. To do so, our protocol can be applied to a different system with smaller particles and/or less viscous background fluid so that intermediate Pe can be accessed at a reasonable shear rate (the system in our paper has a $Pe \sim 10^5$ at a shear rate of 1 s^{-1}). We hypothesize that in this intermediate range of frequencies where the timescale for Brownian forces to homogenize the system is comparable to the advective forces, the Brownian rearrangement will significantly affect how the particles pack and strongly alter the contribution of the Brownian and contact contributions to the total stress. The exact interplay between advective and Brownian forces remains unclear for this intermediate range of frequencies, and experimentally tracking how the Brownian and contact stresses evolve through our protocol can likely provide some intuition of how the microstructure is changing.

Q3: *Is it appropriate to rephrase the discussion on the relaxation time into one on the contribution of each stress term? (Reza Foudazi)*

A3: This is what we do implicitly in the paper. We discussed in the background section that the contact stress decays too quickly to be captured, and that the hydrodynamic stresses go to zero at the point of cessation. Essentially, what is left is the Brownian stress and so the relaxation time we measure is the relaxation of the Brownian stress. At an infinitesimally small time step away from the point of cessation, it is more difficult to disentangle the various stress components. At such small timescales, we will measure not only the decay of the Brownian stress but also the decay of the contact stress and any higher-order nonlinear components from the hydrodynamic stress. The most obvious way to probe a problem that requires such a high time resolution is through simulations. Some of these have been done previously such as in [46] and [49] in our paper. However, even simulations are extremely challenging given multiple simulations have to be run with a small enough time step to reasonably quantify the Brownian behavior. Development of better resolution rheometers and fast 2D imaging of a dense suspension undergoing

shear cessation may also provide us with some idea of how the microstructure is changing after shear cessation.

“AFM as a tool to characterize contact interactions for dense suspensions,” Chiao-Peng Hsu, Shivaprakash N. Ramakrishna, Joydeb Mandal, Nicholas D. Spencer, and Lucio Isa

This talk was associated with [3].

Q1: *How relevant are these individual particle friction experiments to the suspension flow. Could there be phenomena in the suspension flow to amplify or suppress the frictional forces? (Itai Cohen)*

A1: These measurements describe single-particle level contacts and provide microscopic insights into the nature of those contact interactions. In a sheared suspension, where we expect each particle to have multiple contacts, these effects will be amplified; however, colloid-probe atomic force microscope (AFM) friction measurements are carried out in a boundary-lubrication regime, i.e., where the friction coefficient depends very weakly on sliding speed and normal load. In a sheared suspension undergoing discontinuous shear thickening (DST), we know that a broad spectrum of contact pressures as well as relative sliding velocities exist, where hydrodynamically lubricated contacts may coexist with boundary contacts. This calls for further characterization of such contacts under different conditions.

Q2: *How does one know how far from the surface the particle is? (Itai Cohen)*

A2: In an AFM experiment, the zero-separation reference point is determined by performing a force-distance curve. In such an experiment, the cantilever is made to approach toward the surface at a constant speed and the vertical deflection is measured. The zero point is determined as the point at which the approach curve shows nonzero vertical deflection due to interactions with the substrate. More precisely, for hard particles, such as silica, if long-range repulsive forces are present, one observes a change of slope in the force-distance curve upon hard contact, which is used to define the zero-separation. In the presence of attractive forces, an instability occurs upon approach and the cantilever “jumps into contact” before zero separation, showing a negative deflection before hard contact. Here, zero distance is defined as the point where the deflection crosses the zero again upon continuing the approach [33].

Q3: *What information from the AFM measurements can be transferred to the way we describe the different stress contributions? (Emanuela Del Gado)*

A3: The colloid is rigidly anchored to the cantilever, so there is no option to measure the Brownian stress contribution. The method definitively gives access to single-particle contact stress contributions. The measurements can additionally be used to measure the normal components of the hydrodynamic stresses on a particle close to a solid boundary over a broad frequency spectrum. The corresponding measurement of tangential hydrodynamic forces is much more limited.

Q4: *A maximum packing fraction of $\phi_m = 0.4$ would suggest a quite large friction coefficient, much larger than found in AFM experiments. Could there be additional interactions other than frictional contacts? (Romain Mari)*

A4: This is a very good point, to which, frankly, we do not have a definitive answer. Undoubtedly, the values of measured friction coefficients strongly depend on the measuring conditions and on the specific surface-preparation protocols, with large variations found for nominally identical surfaces, e.g., silica, in the presence of small amounts of ions or organic contaminations. What one can robustly compare are relative friction coefficients among different systems measured in a consistent way [33]. In our opinion, this requires a concerted and systematic effort bridging between experiments and numerical simulations to identify a standardized way to measure and reconcile the values employed in simulations with those experimentally measured under well-defined conditions.

Q5: *Can an orthogonal shearing protocol help distinguish between sliding friction and rolling friction?* (Itai Cohen)

A5: Good question, and, again, we frankly do not have an answer for that; however, our naïve answer would be “probably not.” By linear superposition of shear in orthogonal directions, one would be measuring the same kind of response along different directions. This can be very useful to extract how the structure of the suspension under shear, and especially upon DST, affects the shear response. As such, we see the technique as a powerful way to decouple hydrodynamic from contact contributions, but we are not sure as to how it can be used to discriminate between sliding and rolling contacts between particles.

Q6: *Can we engineer particle surfaces to constrain sliding, rolling, and twisting and study whether these different degrees of freedom can be tuned independently?* (Wilson Poon)

A6: This is an essential point that our group is actively working on, and we believe that it can be achieved by careful combinations of surface structuring and surface-chemical functionalization [34]. Starting from the case of spherical particles, there are ways to modify their surface topography by growing asperities of different morphologies, which may or may not allow different kinds of relative motion. The addition of surface coatings with tunable adhesions offers an orthogonal way to engineer relative motion and a combination of both approaches offers great promise.

“The Darcytron: A pressure-imposed device to probe the frictional transition in shear-thickening suspensions,”

Cécile Clavaud, Bloen Metzger, and Yoël Forterre

Q1: *Is the friction here coming from the electrostatic repulsion or from an actual contact? And do you see a second transition at even higher pressures?* (Itai Cohen)

A1: Here, friction arises from solid interparticle contacts. At low imposed confining pressure, we find that the macroscopic friction coefficient of the suspension in the quasistatic flow regime ($J \rightarrow 0$) is $\mu = 0.1$; in this case, the suspension behaves as a suspension composed of frictionless particles (with the interparticle friction coefficient $\mu_p = 0$) since the repulsive force between the grains is strong enough to prevent solid contacts. Conversely, at large pressure, the repulsive force is overcome and the macroscopic friction coefficient of the suspension $\mu \cong 0.5$, which is typical of a suspension composed of frictional grains. No second transition at higher normal stress was observed. In fact, we do not expect a second transition as long as the frictional contacts between grains remain of the Coulomb form.

Q2: *Have you considered studying Darcy flows on a larger scale and more heterogeneous flows?* (Morgane Houssais)

A2: No. What we have considered is to extend pressure-imposed measurements beyond the quasistatic flow regime to study the dependence of the suspension friction coefficient μ on P/P_{rep} and also on $J = \eta\dot{\gamma}/P$, thereby investigating the two parameters expected to control rheology of shear-thickening suspensions.

“Experimental test of a frictional contact model for shear thickening in concentrated colloidal suspensions,”

Yu-Fan Lee, Yimin Luo, Scott C. Brown, and Norman J. Wagner

Q1: *Can the sign or magnitude of N_1 help distinguish between sliding friction and rolling friction?* (Safa Jamali)

A1: Thank you for this question concerning the role of various types of contact friction. Our experimental results and those we cite, coupled with a broad range of simulations and theory, indicate that the sign of N_1 can help one to discriminate between micromechanical mechanisms contributing to the shear stress. A deeper understanding of why this is so requires a more extensive elucidation of the microstructure in the shear-thickened state and how this depends on whether enhanced hydrodynamic lubrication or contact friction is operative, which is the topic of a forthcoming paper. Essentially, the mechanistic distinction at the particle level depends on the inherent reversibility of Stokes flow (lubrication) vs the irreversibility of contact friction. In the former, dissipation occurs under both compression and extension, while in the latter a normal load (e.g., compression) is necessary for dissipation. The asymmetry of the latter leads to a positive normal force. Importantly, our experimental results for titania suspensions, where strong van der Waals attractions are operative, demonstrate semiquantitative agreement with the model of Singh *et al.* [6] tested in our work, supporting the notion that a significant normal load is necessary for contact friction to be operative. The distinction between sliding and rolling friction was not explored in our published research, but as both require a normal load to be operative, one might reasonably anticipate that the contribution to N_1 will be qualitatively similar, but with quantitative differences. A very recent publication describes a simulation that explores how rolling friction can enhance shear thickening by “interlocking” such that force chains can be stabilized relative to particles with only sliding friction [37]. The model predictions show that enhanced rolling friction leads to a more positive N_1 , a more anisotropic force chain structure, and lower particle concentration required for jamming. These results logically follow earlier simulations showing how constraints on particle rolling affect colloidal gel rheology [36], and how the structure imparted by these constraints directly contributes to the rheology. Our comparison of theory and experiment (Fig. 8 of our paper) for the effect of contact friction on the shear-thickening jamming fraction shows that the measured volume fractions for jamming are lower than predictions of models based on sliding contact friction, but not nearly so low as predicted by Singh *et al.* for infinite rolling friction. Unfortunately, Singh *et al.* do not compare their simulations to experimental data including N_1 , and so we

await more model results in order to test their proposed mechanism. It would be intriguing if the experimental data for titania suspensions shown in our paper [Figs. 6(b) and 6(c)] could be better described quantitatively if some measure of rolling friction were added to the contract friction considered in the original model of Singh *et al.* [35].

“Tuning the shear-thickening response of fumed silica suspensions,” *Philippe Bourriane, Vincent Niggel, Gatiien Polly, Thibaut Divoux, and Gareth H. McKinley*

This talk was associated with [7].

Q1: *Are the silica aggregates in your system deformable? And for the hydrophobic and hydrophilic particles, are the aggregate shapes and fractal dimensions different, and if so, how can one make comparisons of the rheology in the two cases?* (Reza Foudazi)

A1: We study shear-thickening suspensions made of four distinct fumed silica particles, each consisting of mean aggregate sizes of $D \approx 300$ nm. These aggregated particles are composed of rigid spherical silica nodules of size $R_u = 10$ or 25 nm, which are subsequently chemically treated to be hydrophilic or hydrophobic. These nodules are fused together permanently during the flame synthesis [37]. Due to silica’s intrinsic rigidity, these sintered aggregates are thus not deformable and unbreakable over the range of applied stresses investigated in our work. Moreover, the fumed silica particles’ shape depends on the size R_u and the number N_u of elementary nodules in each aggregate. We have also taken multiple SEM pictures of individual particles to characterize the parameters R_u and N_u for each batch of particles. The SEM pictures confirm that by coating the natively hydrophilic fumed silica particles by silanization, we can dramatically change the surface chemistry (making them hydrophobic) without affecting the particles’ overall shape to the subnanometer silanized layer. The invariant shape of the aggregated particles during the hydrophobization process allows us to compare carefully the effect of just changing surface chemistry on the degree of shear-thickening. By picking another batch of hydrophilic and hydrophobic fumed silica particles of different primary nodule size R_u , we were also able to change the effective nanometric roughness or topography of our “rough” particles. To compare our measurements, we indeed need to consider the change of morphology of the aggregated particles that results from changing the nodule size R_u . Our paper proposes a model that allows us to predict the onset of continuous shear-thickening based on the size R_u and the number N_u of nodules that constitute the fumed silica aggregates. Our model can predict the experimental change observed in our rheological data.

Q2: *You state that hydrogen bonds are essential for DST. Is this claim general or only for the suspensions explored in your study?* (Edward Ong)

A2: By modifying the particles’ surface chemistry, we indeed argue that hydrogen bonds are essential to achieve DST in suspensions of fumed silica over the range of stresses and volume fractions investigated in our study. Very surprisingly, these suspensions exhibit continuous shear thickening (CST) at relatively low volume fractions, and this arises from

the strongly aspherical and fractal-like geometry of the fumed silica aggregates. By defining an interparticle distance based on the geometrical features of a single fumed silica aggregate, we are indeed able to demonstrate that CST begins when the distance between particles is comparable to the largest dimension of the aggregate, paving the way to solid contacts. This observation does not depend on the surface chemistry and is only set by the particle morphology. By increasing the volume fraction, we reduce the interparticle distance and allow stronger hydrodynamic interaction and frictional contacts. However, we only observe DST behavior when the particles are hydrophilic. In the presence of reversible short-range attractive forces such as hydrogen bonds (<1 nm), the frictional contacts can be enhanced and maintained, amplifying the magnitude of the shear-thickening transition and eventually leading to DST. We indeed report DST for extremely low volume fractions of hydrophilic particles (i.e., below 10%) in clear contrast with existing theories [38] and other typical observations of DST usually associated with dense suspensions [39]. By contrast, hydrophobic particles (which do not support hydrogen bonding interactions) of the same morphology and volume fraction do not exhibit DST behavior. We thus believe that hydrogen bonds are essential in our silica suspensions due to our aggregated particles’ geometry and specific sizes. Similarly, hydrogen bonds have also been reported as a key ingredient to enhance shear-thickening behavior in other systems such as high-volume fraction suspensions of spherical particles [40]. However, based on the available datasets, we cannot generalize the critical importance of hydrogen bonds to achieve DST in all suspensions. Indeed, in the absence of hydrogen bonds (i.e., for hydrophobic fumed silica), we still notice a weak but still measurable shear-thickening behavior. Similar findings have been reported for other suspensions in the absence of hydrogen bonds [41]. Even though it is unclear whether such systems are ever able to achieve DST, we may expect it to increase the magnitude of the shear-thickening transition by increasing the volume fraction further. However, this might require more sophisticated physico-chemical modifications to the particle surfaces.

Q3: *Particle anisotropy is an important factor and the suspensions which shear thicken at relatively low volume fractions often have high aspect ratios. What is the aspect ratio in your system and can you use this to define an effective volume fraction?* (Vikram Rathee)

A3: The morphology of the fumed silica particle indeed sets the critical volume fraction to achieve shear thickening. The size R_u and the number N_u of individual nodules which comprise one fumed silica aggregate control that transition. These parameters also describe the range of possible aspect ratios of a particular aggregate particle, but, given the sintered aggregates’ irregular fractal-like nature, the aspect ratios of individual particles can vary significantly. We develop a simple geometric scaling based on average interparticle distance (compared to the largest linear dimension of the particle), which allows us to predict the critical volume fraction for the transition to CST. Our scaling captures the basic features of that transition correctly. Due to the irregular geometry of our aggregate particles, we have chosen to build our

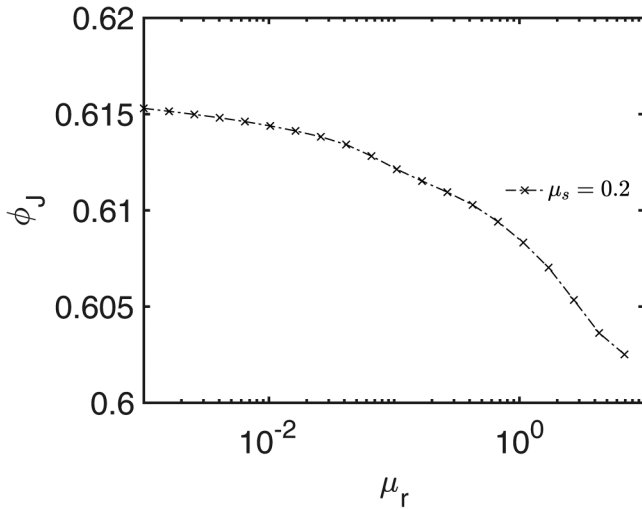


FIG. 1. The dependence of jamming volume fraction on rolling friction for $\mu_s = 0.2$.

scaling model using the average interparticle distance rather than on an effective hydrodynamic volume fraction (its 3D analog). However, to go further and predict the magnitude of the shear-thickening transition, it would be necessary to adopt a more complex modeling approach, calibrated with careful experiments with particles of controlled morphology and/or aspect ratio [42]. Such approaches might be a way to connect our experimental results, which show the onset of DST at very low volume fractions with existing theories designed for regular spherosymmetric shapes [38].

“Shear Thickening and Jamming of Dense Suspensions: The ‘Roll’ of Friction,” *Abhinendra Singh, Christopher Ness, Ryohei Seto, Juan J. de Pablo, and Heinrich M. Jaeger*

This presentation was associated with [6].

Q1: *How do correlation lengths in sliding vs rolling frictional systems compare when evaluated at equal distance from jamming?* (Jurriaan Gillissen)

A1: The system with both sliding and rolling friction compared to the one with only sliding friction will have a larger correlation length when evaluated at the same distance from the jamming point. As an example, the velocity correlation length at large stress for $\phi = 0.45$, $\{\mu_s, \mu_r = 1, 0.5\}$ is 3.5, while that for $\phi = 0.56$, $\{\mu_s, \mu_r = 1, 0\}$ is around 1.5 (as shown by Ness *et al.* [43]). Here both correlation length values are given in terms of the diameter of the small particles used in the simulations. We have not systematically explored the behavior of other correlation lengths with respect to sliding/rolling jamming points, though this would be an interesting avenue for further study. These presumably diverge at the relevant ϕ_J , but we do not have reason to suppose that the divergences would be the same for sliding and rolling dominated systems. On a related note, we also found the scaled first normal stress difference for $\phi = 0.45$, $\{\mu_s, \mu_r = 1, 0.5\}$ to be larger compared to $\phi = 0.56$, $\{\mu_s, \mu_r = 1, 0\}$ as reported in our previous works [35,44,45], again suggesting that the physics of the divergences close to jamming are distinct. The positive large value of N_1 implies a transient elastic network.

Q2: *Does the finite size of the system affect the results in the simulations with high rolling friction coefficient?* (Farhang Radjai)

A2: Here, we present results with $N = 2000$ particles, and we agree that there might be some finite size effects, especially at large stresses. The system analyzed here is around 12.6 particle diameters in size along each side, with the correlation length being around 7. For a more detailed study of the scaling behavior very close to jamming points, it would be necessary to use considerably larger systems.

Q3: *For purely hydrodynamically interacting smooth particles in Stokes flow with no Brownian motion or contact forces, the system cannot be steadily sheared when the volume fraction is above a maximum value well below the random loose packing [46]. The gaps all go to zero. Is this related to the rolling friction discussed?* (John Brady)

A3: No, the problem encountered by Ball and Melrose is not rolling friction related. An important point to consider is that the rolling friction we have studied is for particles in contact, while that studied by Ball and Melrose is for particles interacting via lubrication interactions. The singular behavior as observed by Ball and Melrose and rolling friction is not related. Importantly, for the case of perfectly smooth particles, rolling friction is expected to be zero or very small. As assumed in our previous works [44,45,47,48], we regularize the lubrication singularity. For the case of particles with rough surfaces, some rolling friction is expected.

Q4: *Could flow type (e.g., an irrotational flow, which has nominally no vorticity) be used to probe flows in which rolling friction is presumably less important?* (Gareth McKinley)

A4: This is an interesting question and worth investigating. The microstructure formed in, for example, planar extensional flows is symmetric across the compressional and extensional axes, while the vorticity in simple shear flows distorts such microstructure. Nevertheless, the rheological behaviors of planar extensional and simple shear flows are almost indistinguishable in dense suspensions with only sliding friction [48,49]. However, since rolling friction stabilizes contacts against buckling, those suspensions can become jammed with more tenuous structures at lower volume fractions. Since longer structural units are sensitive to force moments, the flow-type dependence may be more noticeable with rolling friction.

Q5: *In your simulation, if you completely remove the sliding friction, does the rolling friction matter?* (Yoël Forterre)

A5: In the absence of sliding friction, particles do not rotate following oblique contacts, therefore the rolling displacement used in the pseudoforce calculation is zero. Consequently, in the absence of sliding friction, adding rolling friction (at least in our formulation) has no effect. Meanwhile, for relatively small sliding friction, e.g., $\mu_s = 0.2$, there is a very weak dependence of ϕ_J across a broad range of μ_r (Fig. 1).

“A hydrodynamic model for discontinuous shear-thickening in dense suspensions,” *Mu Wang, Safa Jamali, and John F. Brady*

Q1: *Is there a macroscale experiment that the authors could suggest to evaluate this model, e.g., acoustic perturbations or for orthogonal shear?* (Itai Cohen)

A1: It is challenging to design macroscopic experiments to differentiate the underlying mechanisms for the onset of DST, as we have illustrated through the toy examples in Sec. IIA in the paper. Different underlying mechanisms may give rise to identical macroscale rheological responses. Therefore, to test the model, there must be a component to evaluate the microscopic configurations of the suspension. A negative first normal stress difference (N_1) indicates that hydrodynamic interactions (HIs) are dominant. However, a positive N_1 does not mean that HI are not important. N_1 is very sensitive to the detailed microstructural arrangement of particles and the precise nature of the interparticle interactions, both hydrodynamic and nonhydrodynamic. Slight modifications of these interactions can change the sign of N_1 even though HI dominate the shear stress. Flow cessation, reversal or other perturbations to the microstructure have the challenge of being able to resolve time scales short compared to those that determine the structural relaxation. The shear-thickened state is held together by a network of contacts and breaking only a few can completely destroy the load-bearing structure. The fundamental time scales arise from the interparticle forces and Brownian motion. For interparticle forces, $\tau_F \sim 6\pi\eta a^2/F$, where η is the solvent viscosity and a is the particle radius. F is the magnitude of the interparticle forces at “contact.” For Brownian motion, $\tau_D \sim 6\pi\eta a^2/k_B T/\delta$, where δ is the contact length associated with the interparticle force F . While these are the characteristic time scales, it must be appreciated that there will be a distribution of contact distances δ and only a tiny fraction need to relax to drop the stress by orders of magnitude.

Q2: *Why is there a large difference in N_1 between Stokesian Dynamics and Dissipative Particle Dynamics simulations?* (Jurriaan Gillissen)

A2: There are several reasons for the large differences in the first normal stress difference computed by the two methods. First of all, the effects of surface asperities are treated differently in these two methods, despite the fact that these effects all arise from HI. In dissipative particle dynamics (DPD), the surface asperities are modeled as explicit inclusion particles distributed randomly on the surface of the colloidal (large) particles. For this work, only the surface coverage, not the inclusion sizes, changed. In Stokesian dynamics (SD), the surface asperities are modeled implicitly in a mean-field fashion such that they qualitatively alter the divergence of HIs when two particles approach each other. The differences in modeling surface asperities is the primary reason for the differences in the normal stress differences. Second, the solvents are treated differently between DPD and SD. Specifically, in DPD, the solvent particles are present explicitly in simulations to preserve long-range interactions. In SD, the solvents are implicitly treated through the grand mobility/resistance matrices. When the particles are close to each other, the solvent particles in DPD may be depleted between the two surfaces, and may introduce errors in evaluating the HIs. In this work, the significant size differences between the colloidal particle and surface asperity particles make accurate capture of HI challenging. On the other hand, in SD there is no explicit solvent, solvent particle depletion is not an issue. This may, to a lesser degree, contribute to the

normal stress differences. Finally, in our study, we never matched repulsive forces or the background viscosities between DPD and SD. Therefore, we do not expect the normal stress differences to match.

Q3: *What is the physical basis for the modified form of the lubrication as a function of gap width?* (Edward Ong)

A3: The physical intuition and rationale for the modified form of the lubrication is described in Sec. IIB in the paper. Essentially, our physical intuition is that surface asperity on colloidal particle qualitatively changes the sliding motion hydrodynamic force from a weak divergence proportional to the logarithm of the gap spacing, $\sim \log(1/h)$, to a strong divergence proportional to the inverse of the gap spacing $\sim 1/h$. In addition, the effect of the surface asperity is assumed to be local: this leads to a form that becomes exactly zero in its value and its first derivative when the gap spacing is at h_0 .

Q4: *It appears that “ α ” is, in part, due to a squeeze mode between “bumps” on the particle surface. Have you tried to estimate what “ α ” should be based on the local curvature of the bumps and compare to your fits of data?* (Nicos Martys)

A4: We have not tried to make such an estimate yet. For the SD study, parameter α in Eq. (6) in the paper can be interpreted as a function of the local curvature of the bumps. However, a direct correspondence between α and the local curvature has not been established as the parameter characterizes the hydrodynamic force instead of the local geometry. On the other hand, the DPD simulations do provide an estimation of the local curvature, as both the inclusion size and coverage can affect the results. In this work, only the surface coverage, not the inclusion size is varied. It should be noted that while in this work monosized spherical bumps were modeled using the DPD scheme, one can generate arbitrary decorations, sizes and curvatures of asperities by incorporating bumps of different sizes to construct a composite geometry.

Q5: *Have you done simulations of shear reversal?* (Jin Sun)

A5: We have not run shear reversal simulations but are planning to do so in the near future. These simulations will inform the time scale associated with the relaxation of hydrodynamic stresses in the shear-thickened system and are very interesting. The results for such flow protocols could improve upon building macroscopic flow protocols to identify dominant microscopic interactions. We would look to investigate the time scales identified in our response to Q1.

“Roughness induced shear thickening in frictional non-Brownian suspensions: A numerical study,” Rishabh V. More and Arezoo Ardekani

Q1: *Your model combines both friction coefficient and surface roughness. Can the two parameters be decoupled?* (Yu-Fan Lee)

A1: The particle surface roughness is a geometrical property while the coefficient of friction is a material property; however, the friction coefficient is not a completely independent parameter from surface roughness. Theoretically, lubrication interactions should prevent perfectly smooth particles

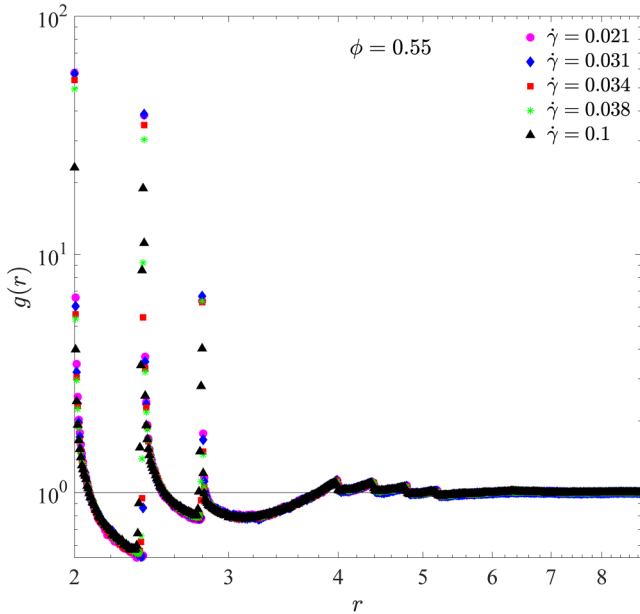


FIG. 2. Angularly averaged pair-distribution function for shear rates spanning the dimensionless “critical” shear rate of 0.0315 at the onset volume fraction of $\phi = 0.55$ display only slight differences.

from touching. But particles come into contact via irregularities on their surfaces. It is only when these contacts take place that the friction between the particles is activated. Hence, the particle roughness is a prerequisite for friction. Also, the coefficient of friction is highly dependent on the surface properties of the particles and increases with increase of the surface roughness value [3]. We have also shown that a roughness-dependent coefficient of friction can explain the experimentally observed rise in the suspension viscosity with increasing the roughness size [50]. Earlier numerical models which assumed a decoupled or a constant coefficient of friction could not explain this rise in the suspension viscosity with the particle roughness. In addition, it has been shown that the coefficient of friction depends on the normal load between the particles [51,52]. The normal load, in turn, depends on the roughness deformation and the roughness size/distribution, e.g., via Hertz’s law. Hence, the friction coefficient is highly dependent on the surface roughness of the particles along with the particle material and the two parameters cannot be decoupled.

“Fluctuations at the onset of discontinuous shear thickening in a suspension,” Omer Sedes, Abhinendra Singh, and Jeffrey F. Morris

Q1: Do the radial distribution functions, $g(r)$, show the power law divergence that is associated with jamming of dry grains? (Bulbul Chakraborty)

A1: In the vicinity of the onset of DST, we see no distinctive changes in the pair-distribution function, with either volume fraction or shear rate. This point, consistent with the findings reported by Mari *et al.* [44], is illustrated by the plot of angularly averaged pair-distribution function shown in Fig. 2 at $\phi = 0.55$ from the thesis of O. Sedes [53]; this is the volume fraction associated with the apparent critical point for the microscopic parameters of the simulations presented in the

paper. Note that for $\phi = 0.55$, the dimensionless shear rate for which DST is seen is $\dot{\gamma} = 0.0315$. The constraints of packing in the suspension of half (by volume) particles of relative radii 1 and 1.4 seem to control the observed structure.

Q2: There are three potential sources of power law fluctuations: (1) the constraint of shearing, (2) proximity to a critical point generically, and (3) jamming fluctuations (which may or may not be the same as 2). Do you suggest that there are other additional sources as well? And do you have an interpretation of which one is responsible for your fluctuations? (Peter Olmsted)

A2: Our data indicate that the fluctuations in stress, which are peaked around a localized point in the ϕ – σ plane, are due to proximity to the apparent critical point, the source (2) in this list. The constraint of shearing (1) would apply at any condition, and while fluctuations are a natural feature of the behavior of suspensions, these show no singular features away from (ϕ_c, σ_c) . The behavior we report is certainly distinct from jamming, source (3) in this list, as the fluctuations are reduced at large stress (large shear rate) for systems below the frictional jamming fraction; the localization of this intense fluctuation region with respect to both solid fraction and stress in the flow-state diagram indicates this is distinct from jamming of the whole material.

Q3: Did you study the nature of the fluctuating deformation field and associated microstructure? (Jurriaan Gillissen)

A3: We have not made a systematic examination of the kinematics associated with the fluctuations. The appearance of long-range correlations in velocity suggestive of pseudo-solid rotation found in SD simulation, described in a thesis by Kulkarni [54], were influential in motivating the development of the lubricated-to-frictional rheology used in our paper. The point is well worth study.

Q4: Since there exist multiple constraints, there must be a point at which the suspension expands as the particles pass each other. Can simulations reproduce this dilation effect? (Yu-Fan Lee)

A4: The simulation results presented here are under constant volume. Dilation of the particle phase requires some mechanism to allow the fluid to flow in: In simulation this can be done artificially for the triply periodic conditions we have studied, but this is not captured in our algorithm. See Peyneau and Roux [55] for a method with variable volume fraction. Since the volume is constant, under fixed shear rate, the stress responds as necessary to achieve the imposed conditions. In simple terms, one can think of the particle pressure as indicative of a tendency of the particle phase to dilate; similarly, a positive first normal stress is typically termed a dilatant response, as the structures developed in the material apparently lead to the outward thrust on the driving surfaces in the gradient direction.

“Localized transient jamming in discontinuous shear thickening,” Vikram Rathee, Daniel L. Blair, and Jeffrey S. Urbach

Q1: Does the suspension shear thicken and then undergo instabilities where the stress pushes on the soft boundary, consequently releasing the cluster from the confining stress? (Itai Cohen)

A1: This is a very good question, and it is hard to know for certain the role of boundary compliance in the high stress fluctuations. However, all of our observations to date suggest that the boundary stress behavior is similar when the polydimethyl siloxane (PDMS) stiffness is changed, and that fluctuations in the bulk rheology and local suspension dynamics (from imaging) are similar when we have a hard (glass) boundary. The compliance of the boundary certainly could affect the detailed evolution of high stress fluctuations, but we expect that there would not be a qualitative change. Note also that the high stress regions that we report can survive for hundreds of strain units, so the solidlike phases (SLPs) are quite stable, suggesting that boundary dynamics are not playing a central role in the instability.

Q2: *Your argument for CST involving high-viscosity regions, and DST requiring transient jamming suggests that microscopic rigidity beyond the scale of a single particle is the physical issue. Is this how you interpret the behavior?* (Jeff Morris)

A2: Yes, we do think our results indicate a mechanism of this nature. Our measurements both in the CST and DST show a clear spatial extent which is either comparable to or larger than the gap size between the shearing plates, indicating that the behavior can only be explained by dynamics on a length scale that is large compared to a single particle. One possibility is that boundary confinement is playing a central role in driving the transition to the high viscosity or jammed phases. For example, perhaps gap-spanning fluctuations get amplified by feedback from the boundaries, while smaller fluctuations normally dissipate.

Q3: *Are the particles in the SLPs that are anchored to the bottom plate observable using confocal microscopy?* (Sam Brown)

A3: We anticipate that they will be observable in direct imaging and have some preliminary evidence that this is in fact the case. There are some technical challenges which we are working to overcome and hope to have robust results soon.

Q4: *Is it plausible that rough particles interlock and hence the force chains stay constrained?* (Abhinendra Singh)

A4: We think it is quite plausible that the particles interlock due to their roughness, and this is in fact what stabilized the SLPs. As mentioned above (in response to the previous question), we anticipate and have preliminary evidence for anchoring of particles in SLPs to the bottom plate. It seems likely that these particles are interlocked (or at least are highly constrained), although it would be hard to say for sure from our measurements.

Q5: *Based on your results, would you suggest that considering large jammed solid domains under flow would be a viable path for continuum models of shear thickening?* (Giulio Giusteri)

A5: That is a very good suggestion, and we do think that including a solid fraction, with some dynamics describing the boundary between the solid and flowing phase, will be necessary to provide a full description of flows in DST. The SLPs that we observe are relatively stable for 10–100s of strain units, so there is a quasisteady state that could be described by a static solid phase but capturing the evolution would require modeling the interface dynamics as well.

“Investigating the nature of discontinuous shear thickening: Beyond a mean-field description,” *Jetin E. Thomas, Abhay Goyal, Deshpreet Singh Bedi, Abhinendra Singh, Emanuela Del Gado, and Bulbul Chakraborty*

Q1: *How do you interpret the phase diagram that you obtain based on the effective forces? And what do the “force clusters” mean in a physical sense? Are those responsible for the CST/DST in any way?* (Poornima Padmanabhan)

A1: The force-tiling representation (Figs. 4 and 5 in the paper) takes every grain and maps it on to a polygon (in 2D) that is obtained by laying down the interaction forces of that grain head to tail. So, when we see clustering of vertices of this tiling, as in Fig. 10 of the paper, that indicates a microphase separation with regions of small forces (predominantly from lubricated contacts) embedded among large-force contacts. Therefore, the clustering diagram in Fig. 10 indicates that the CST-DST transition is accompanied by more pronounced clustering since we are in the CST regime in the left panel and in the DST regime in the right panel. This is especially true at low T . Since we do not yet have a mapping of the temperature in the molecular dynamics simulations to a corresponding intensive variable in the suspensions, the implications of the change in clustering as temperature is increased are not completely clear to us. In our earlier work [56], the phase diagram was obtained by tracing out the locus of points where $d\dot{\gamma}/d\sigma = 0$. We used the effective potential obtained from the pair correlation in force space, discussed in our current paper. This pair correlation function lets us construct a generating function, analogous to the partition function in equilibrium statistical mechanics. From this, we compute the average stress anisotropy, μ . We then used a generalization of the Boyer–Guazzelli–Pouliquen [57] suspension rheology to a rate-dependent form that relates the viscosity to μ to construct the phase diagram. From both sets of analysis, what is clear is that there are well-defined changes in the force-tiling patterns that reflect a collective reorganization of forces as a suspension transitions from CST to DST. The force-tiling representation thus promises to be one that can be fruitfully exploited to construct a statistical mechanics framework for these nonequilibrium transitions.

Q2: *Given the analogy with Gauss’s law and the electrostatic free energy function, is it possible to understand the stress interactions as long-range correlations with an inverse of distance scaling behavior?* (Vikram Jadhao)

A2: Yes, the stress-correlations are long ranged and go as $1/r^{d-1}$, in d -dimensions. This is a consequence of Gauss’s law. For this tensorial Gauss’s law, however, these correlations are not isotropic and there are distinct anisotropies predicted by the theory that we have confirmed in simulations and experiments. For more details please see [58].

Q3: *For Gauss’s law to hold you need far-field behavior going to zero. Does your gauge theory lead you to long-range correlations? and if so, what are your thoughts on the far-field limit? Also, how far can you extend the analogy between the local force balance and the electrostatic energy? In another word, is it possible not to have a local force balance, and still have overall force balance imposed?* (Buddhapriya Chakrabarti)

A3: The gauge theory does lead to long-ranged correlations of the stresses, and the far-field behavior of the correlations indeed goes to zero. The local force and torque balance are essential for constructing the gauge theory. Overall force balance is not enough. The statistical mechanics that we construct is analogous to that of frustrated magnets at zero temperature. We assume that all microstates that satisfy both the local constraints and the boundary conditions imposed are equally likely in our zero-temperature ensemble. This partition function translates to the pure-gauge Lagrangian of the $U(1)$, vector charge theory. For more details please see [58].

“Stress fluctuations and shear thickening in dense granular suspensions,” *Qin Xu, Abhinendra Singh, and Heinrich M. Jaeger*

Q1: *Is relative viscosity sufficient for considering the effects of the background fluid? Do the hydrodynamic effects of many-body particles have an additional contribution?* (Reza Foudazi)

A1: The relative viscosity of a dense suspension, η_r , characterizes the mean flow resistance to shear. In rheological experiments, η_r is measured by averaging the stress-strain relationship over a certain period of time (Figs. 1 and 2 of the paper). However, the relative viscosity by itself does not reflect the statistical nature of various local stresses in the suspensions, especially frictional stresses at particle contacts which are dynamically rearranging under shear. For this reason, we believe that studying the stress fluctuations of dense suspensions is a valuable approach to unfold the hidden dynamics in shear flow (Figs. 3 and 4). In this work, the measured relative viscosity certainly involves the HIs among many particles. In particular, we found the increase of solvent viscosity can strengthen the lubrication layer between particles such that it reduces the stress fluctuations (Fig. 3) and the degree of shear thickening (Fig. 1).

Q2: *Dimensional analysis suggests that your results require an additional timescale. Is it possible that the high-viscosity fluids used have some non-Newtonian response in the lubrication gaps where the shear rate is extremely high and at least partially extensional flow?* (Jeff Morris)

Follow-up Q3: *What are the ranges of oil molecular weights? The viscosity scales with a linear power in M for $M < M_e$ and grows more steeply for larger molecular weights. This can elucidate possible non-Newtonian effects in the background fluid.* (Peter Olmsted)

Follow-up Q4: *Would polymer chain entanglements provide an additional mechanism of stress dissipation and then damping the viscosity and stress fluctuation?* (Grayson Jackson)

A2: This is a great question. We believe that a possible relative timescale could be the relaxation time of the solvents, and in this case corresponds to the relaxation time of the silicone polymers (λ). A relevant parameter is the Weissenberg number (Wi), which is defined as $Wi = \lambda \dot{\gamma}$ for a given shear rate $\dot{\gamma}$. The Weissenberg number characterizes the ratio of elastic forces to viscous forces. At very high shear rates, it is possible that the elastic forces acting on the polymer chains can be significant so that the chains will be highly stretched to generate a partially extensional flow in the gap. According

to the Oldroyd model, the stretched polymer chains will result in an increase of local N_1 and, therefore, amplify the lubrication effects.

A3: According to the vendor information of PDMS (from Gelest Inc.), the molecular weight of the silicone oil increases from $M \sim 500$ to 20 000 g/mol as the solvent viscosity increases from 10 to 1000 cSt. According to reptation theory $\lambda \sim M^{3.4}$, therefore, the corresponding relaxation time λ will increase by a factor of 10^8 while the shear rate decreases by a factor of 100 for a given shear stress. As a result, the Weissenberg number will increase by 10^6 . Thus, the nonlinear effect of the solvents (silicone polymers) could be significant. The role of solvent nonlinear elasticity in suspension rheology needs to be further studied.

A4: Yes, the experiments in this paper indicate that the elastic stresses induced by long entangled polymer chains can significantly strengthen the lubrication between particles to prevent the frictional contacts. Due to this enhanced lubrication, there are three consequences: first, the degree of shear thickening is weakened (Fig. 1); second, shear stress fluctuations are reduced (Fig. 3); third, the spatial correlation length is decreased (Fig. 5).

Q5: *In standard equilibrium phase transitions, the amplitude of fluctuations can be very small, but the length scale divergence leads to a diverging susceptibility. Is this signature observed in the amplitude of the stress fluctuations?* (Bulbul Chakraborty)

A5: In this work, we do not state that the amplitude of stress fluctuations per se determines the divergence of the length scale. Instead, how the amplitude varies with system size lets us extract the correlation length (see Fig. 4). When the sample size is larger than the correlation length, the width of the stress distribution will decrease with the system size due to averaging (see Figs. 4 and 5). On the other hand, if the spatial length scale is divergent, the force distribution over the entire suspension is correlated so that the width of the distribution becomes independent of the sample size. One example of the highly correlated system is shown by the stress distribution plots in Figs. 4(a1)–4(a3) of the paper.

Q6: *At a shear rate that is too large for the polymer chains, the thickening becomes overwhelmed by the hydrodynamic responses. Did you perform experiments at low enough strain rates that the viscous stresses are not as high as the contact stresses?* (Itai Cohen)

A6: In our experiments, we do not think that the shear thickening is overwhelmed by the solvent viscosity. First, the traces in Fig. 1 are plotted in the form of viscosity (η) vs stress (τ). For high solvent viscosity ($\eta_0 > 1000$ cSt), the shear rates in these experiments are very low ($\sim 10^{-4}$ s $^{-1}$). Second, by normalizing the suspension viscosity η with η_0 , we found that in the plots of relative viscosity η_r , the shear-thickening strength still decreases significantly with η_0 (Fig. 2). Therefore, we believe that the viscosity of the solvent does alter the rheological properties of the suspensions. Finally, we found that the roughened suspension interface due to frustrated dilation disappears with increasing η_0 [Figs. 1(c) and 1(d)]. This feature proves that the highly viscous solvent prevents interparticle contacts.

“Particle dynamics predicts shear rheology of soft particle glasses,” *Fardin Khabaz, Michel Cloitre, and Roger T. Bonnecaze*

Q1: *If the system is above jamming, why would it exhibit the ballistic motion?* (Abhinendra Singh)

A1: Ballistic motion at short time is due to the unbalanced elastic interactions experienced by the particles. At any instant in time, any given particle feels the elastic force of several surrounding particles. These forces are not balanced and the particle reacts by moving ballistically in the direction of net force on it. The ballistic motion ceases when the sustained elastic force, which acts at very short times, vanishes. This is supported by the result that the crossover time from ballistic to diffusive motion and the elastic force decorrelation time are proportional. On larger timescales particle motion becomes diffusive. This scenario exhibits an analogy with the classical Brownian motion in thermally activated suspensions.

Q2: *How do the shear stresses and first normal stress differences increase proportionally? This implies that the particle orientation remains unchanged. In another word, what prevents the shear flow to rotate the microstructure more than what is allowed by the static yield criterion?* (Joseph Peterson)

A2: The particle pair-distribution changes drastically under flow and this gives rise to the shear stress and normal stress differences in jammed suspensions at low and high shear rates. At low shear rates, the particles are distributed more uniformly around a test particle; still we observe asymmetric contact distribution. At a high shear rate, this asymmetry becomes more significant, and the axes of compression and extension are clearly observed. In practice, the shear stresses and first normal stress differences are almost proportional [59,60].

“Distance to jamming dictates shear-thickening strength,” *Shravan Pradeep, Alan Jacob, and Lilian Hsiao*

This presentation was associated with [15].

Q1: *Suspensions that can shear jam otherwise, may not show jamming behavior when measured under a rheometer. How do you tell the difference between these “cannot jam” and “does not show jamming” suspensions?* (Endao Han)

A1: Shear jamming is a function of the applied stress and volume fraction, as shown in a series of state diagrams by Liu and Nagel [61] as well as by Peters *et al.* [62]. To answer the first part of this question, the working definition of shear jamming is a liquid-to-solid transition when a finite shear stress is applied. The second part of this question may be asking a more philosophical question that is related to thermodynamics and kinetics: how does one tell the difference between a glassy system and one that shows jamming on a finite time scale under an applied stress? This is challenging to address experimentally because of observation time scales, but Mari *et al.* [63] had provided an earlier answer to this question. A high-level summary of their simulation study is as follows: glasses comprise of particles in deep energy wells separated by high barriers, but they do not exhibit truly zero vibrational modes. One must then apply an extremely large pressure to cause these states to become truly and mechanically jammed. In terms of experiments, this

could mean using a very sensitive microscope that identifies the mean squared displacement of the particles in the system under absolutely zero applied stress, which may be challenging to obtain in a regular laboratory on the Earth. In the context of our work, we apply a working definition of jamming—the average number of nearest neighbors identified in a quiescent suspension is used to identify the isostatic jamming point for various particle morphologies.

Q2: *Your suspensions continue to shear thicken even upon loss of 50% of particle contacts. Does this suggest that only a “few” contacts are responsible for the chains that carry the load? If so, one can perform simulations and remove particles gradually to see when the stress begins to reduce.* (John Brady)

A2: The data indicate that it is very possible that a suspension loses 50% of its nearest neighbors on average and still exhibits shear thickening. Here, a loss of 50% nearest neighbors in the static structure of a suspension is directly linked to shear thickening. We are currently performing experiments to test if this relation holds for dynamically sheared structures. It is entirely possible for a few of these load-bearing contacts to form percolated networks that are responsible for the suspension stresses, just as a few load-bearing struts are responsible for holding up houses and buildings. Contact between colloids is defined as a finite separation distance accounting for experimental uncertainties including the polymer stabilizer brush, swelling in solvents, as well as size and roughness polydispersity [64]. Furthermore, colloidal clusters exert significant hydrodynamic stresses even if they do not percolate through the system. Our data suggest that when more than 50% of nearest contacts are lost, CST becomes dominant. We would be very interested in seeing future simulation work by others that identifies the role of particle networks in suspension stresses. Ideally, one could start with a shear-thickened state in simulations and begin removing particles from the force chains to measure the change in overall suspension stress. However, this requires careful characterization of the relative strength of percolated force chain structures. Recently, simulations have reported on analyzing such network structures through topological data analysis [65]. Combining snapshots from simulations and experimental rheology would provide important insights into how particle and force networks are correlated.

“Rheology and structure of dense colloidal suspensions in confined flow,” *E. Barcelos, S. Khani, A. Lee, J. Peet, and Joao Maia*

Q1: *For dense suspension Poiseuille flow, is there a need to resolve long-range HI, beyond simply conducting lubrication hydrodynamic simulations?* (Jurriaan Gillissen)

A1: In effect, the addition of long-range hydrodynamic force to the model would make it more physically realistic. However, the addition of the term would increase the model complexity and most importantly, the computational cost. Since our system of interest are dense suspensions in which short-range lubrication forces display a major role in the interactions, we choose to only use lubrication, assuming that in this type of system, hydrodynamics can be fairly represented, as has been done by several other groups [46,66].

Q2: *How do you simulate the walls and model the particle-wall interactions? Have you observed lubrication layer formation due to particle migration? If you model the wall as frozen DPD particles, that means there are DPD friction and random forces between the mobile particles and the wall particles?* (Yanwei Wang)

A2: The walls are simulated as a double layer of frozen stationary DPD particles that are able to interact with the free particles in the system. For a more detailed explanation, please see [67].

Since the wall particles are made of soft DPD particles, the interactions take place using the same standard DPD forces. In this case, however, the r_{ij} , which is the center-center distance, is replaced by an h_{ij} term, representing the center-to-surface distance. As pointed out, since the walls are made of DPD particles we do account for dissipative and random forces between particle-wall interactions. We studied a number of parameters that affect our system, and depending on the choice of them, we do see particle migration, which can be toward the center of the box or the walls.

“Impact induced hardening in dense frictional suspensions,” Pradipto and Hisao Hayakawa

This talk was associated with [17].

Q1: *Could you elaborate on how is the plug retained without an apparent shear stress?* (Itai Cohen)

A1: If force chains are percolated, no shear stresses are needed to sustain plugs or dense regions. The process we consider is that an impactor ball is falling down driven by gravity, and thus, the impactor presses the suspension liquid we consider. Then, the normal stress increases in the vertical direction and force chains along this direction are percolated from the surface to bottom plate. Only the normal stress is important in this process.

Q2: *Are your results sensitive to the choice of the two fluid models used in the simulations? Would using a phase field or Cahn–Hilliard model coupled with the lattice-Boltzmann method (LBM), instead of a free surface LBM, change the outcomes?* (Chaithanya K. V. S.)

A2: We believe that we can combine a phase field or Cahn–Hilliard model with a suspension LBM model, though the implementation is not easy. In our case, the air phase is regarded as a vacuum, while if you adopt the phase field model, the air phase and the liquid phase can be continuously changed as in the case of van der Waals gas. The advantage to use this model is that the model includes the surface tension between the liquid and air phases, while our model does not. Therefore, to use the phase field model will improve upon our model, because our model cannot use an ideal density-matching between the liquid and the suspended particles due to the absence of the surface tension.

Q3: *Do force chains necessarily go all the way down to the bottom of the geometry? or can one alternatively envision the plug sheared with respect to the rest of the fluid?* (Itai Cohen)

A3: As answered in our response to the first question, this flow is unrelated to shear stress. Therefore, the percolation of force chains is necessary to sustain the impulse of the

impactor. Since we use a slippery wall, to reach force chains to the bottom wall is necessary, but if we use bumpy boundaries, the impulse can be sustained by force chains that reach the sidewall.

Q4: *Could you comment on whether the rebound is an inertial effect or due to elastic forces between grains?* (Jurriaan Gillissen)

A4: The rebound is the result of an inertial effect. Imagine, if we place a ball on an elastic body without impact speed, the ball and elastic body can be oscillated, but there is no possibility to rebound. To rebound the ball needs the impact speed.

“Soft and highly sensitive pressure sensor arrays for a local normal stress measurement in complex fluids,” Anaïs Gauthier, Mickaël Pruvost, Olivier Gamache, and Annie Colin

This talk was associated with [68].

Q1: *Is the measured pressure in your results a normal stress difference measured by the parallel plates or the actual pressure?* (Peter Olmsted)

A1: As in the work of Dbouk *et al.* [69], we measure $-\sigma_{zz}$. The equation of motion within the fluid is expressed as a function of σ_{zz} and the two normal stresses only: $\partial\sigma_{zz}/\partial r = (\partial N_2/\partial r) + (N_1 + N_2)/r$. This equation is integrated with respect to r , with boundary conditions $\sigma_{rr}(r = R) = -N_2(R) + \sigma_{zz}(R) = P_c$, with P_c being the capillary pressure due to the meniscus at the edge of the geometry. Since all sensors are set to zero at the beginning of the experiment (at zero angular velocity), this preload is already taken into account, as well as P_c . Finally, the “pressure” measured by the sensor is: $P(r) = -\sigma_{zz}(r)$.

Q2: *Could you comment about the relationship between your measurements and other measurements of local stresses (such as from Rathee *et al.* [11])?*

A2: In the work of Rathee *et al.*, the stress which is easily measured is the shear stress. Here, on the contrary, our sensors are sensitive only to the normal force and not to the shear force. Indeed, while the sensors are particularly sensitive to the applied pressure, they do not react to shear stress. We demonstrate this by measuring the sensors capacitance when shearing silicone oil with viscosity 100 000 cSt. At the stresses considered in this experiment, silicone oil is a Newtonian fluid, with a constant viscosity and no measurable normal stress. While the applied shear stress varied over 5 orders of magnitude, the sensors capacitance remained constant.

Another important difference with the work of Rathee *et al.* is the spatial resolution of the measurement. Using a surface 100 times softer than ours (15 kPa) compared with our measurement surface (the modulus of the piezocapacitive foam alone is 1.6 MPa) and a confocal microscope, they map the stress over less than 1 mm², which is approximately the size of a single electrode. However, our setup allows us to get a comprehensive picture of the flow. Our system is close to the one of Dbouk *et al.* [69]. The use of soft sensors is, however, much easier than the use of commercial pressure sensors with membranes. The spatial resolution of our setup is reduced to 0.5 mm compared to 1 cm.

Q3: *Since the aggregate is relatively large, the velocity of this traveling aggregate becomes comparable to the rotation rate of the plate. How important is the radial inhomogeneity of the shear flow and does the relative magnitude of these velocities play a role?* (Vikram Rathee, Prateek Sehgal, Heinrich Jaeger, and Gareth McKinley)

A3: Aggregates of the same nature were evidenced in a Couette cell [70]. The velocity of the aggregate in both geometry (Couette and plate plate) was close to half of the velocity of the rotor. We do not notice the variation of the velocity of the aggregate along the radius of the plate in plate plate geometry.

Q4: *Reversing shear and going at exactly the same shear rate in counterclockwise vs clockwise could help clarify whether the structures observed are quasistatic or relax, diffuse away, and then build up again. Have you considered changing the direction of rotation in your experiment?* (Gareth McKinley)

A4: We have not done this experiment. However, these aggregates relax very easily. They disappear as soon as the stress is reduced below the shear-thickening transition stress.

Q5: *Can you comment on the nature of the high stress aggregate? Are you observing the same group of particles traveling in the surrounding medium or the stresses that propagate across different regions of the suspension?* (Ryan Poling-Skutvik)

A5: A solid part will roll and advance with a velocity equal to the half of the top plate. This is not what we measure. We thus believe that we watch stress waves propagating across different regions of the suspension.

Q6: *Could you comment on the evolution of the stress and pressure as a function of time?* (Bulbul Chakraborty)

A6: The signals measured by the rheometer show fluctuations with time (<25%) but are very noisy. The signals of pressure measured by the small sensors are periodic and display peaks. The peaks suggest the presence of the aggregate. They are associated with localized and very high normal stresses: for a 41% corn starch suspension and a shear stress equal to 150 Pa, the peak pressure is seven times higher than the mean pressure obtained through the force sensor of the rheometer.

Q7: *How do your observations change if you leave the gap to be free to readjust?* (Lucio Isa)

A7: We performed the same experiments with softer surfaces and measured that the aggregates do not form.

“Dilatancy in dense suspensions of model hard-spherelike colloids under shear and extensional flow,” Ricardo J. E. Andrade, Alan R. Jacob, Francisco J. Galindo-Rosales, Laura Campo-Deaño, Qian Huang, Ole Hassager, and George Petekidis

This talk was associated with [18].

Q1: *How do you obtain the dependence of N_1 and dilatancy over time and could you comment on similarities between the time series you obtain and time series of N_1 in simulations? Could you also comment on the origin of differences in N_1 for different types of particles, and would it be possible that the negative values of N_1 for small particles are due to caging effects or other Brownian effects?* (Lilian Hsiao, Rahul Chacko, and Yu-Fan Lee)

A1: Shear and normal stress are measured during start-up experiments (see Figs. 5 and 6 of the paper), while dilatancy effects are followed by direct observation of the sample (see Fig. 7). N_1 is identified with σ_N only in the absence of dilatancy (and/or slip) and is determined, as shown in Fig. 6 (at the point depicted by a star) prior to the onset of dilatancy. In this sense, the full time dependence of N_1 cannot be probed throughout the start-up tests as beyond the point where dilatancy sets in the normal force measured by the rheometer cannot be used to determine N_1 . Consequently, normal or shear force fluctuations seen at large strains (Fig. 6) cannot be identified with shear stress or N_1 fluctuations detected in simulations (see Sedes *et al.* [10]) or experiments (see Lootens *et al.* [71]). The main reason we did not observe shear thickening in the small particles is that the maximum Pe (or stress) reached was smaller than the critical one where DST was observed for the other two (larger) poly(methylmethacrylate) (PMMA) particles (see Fig. 3). Therefore, in this regime, Brownian effects are still dominant. In addition, we cannot exclude the fact the smaller particle might also appear slightly softer due to proportionally larger stabilizing polymer brush.

Q2: *How do you extract information from the CaBER measurements, and are there possible rate dependencies and changes in the size of the filament?* (Reza Foudazi)

A2: In CaBER experiments, the sample is stretched from h_0 to h_f in a certain time (see Table 1), resulting in different stretching rates, and then the time evolution of the filament width $D_{\text{mid}}(t)$ is followed. Different types of behavior are then directly visualized (see Figs. 8, 9 and 11) at different stretching rates: at low rates samples behave as liquids, while at high rates they exhibit shear thickening and brittle fracture (see section B). The initial aspect ratio of the sample was fixed to a rather low value ($\Lambda_0=0.75$) due to low surface tension, introducing non-negligible shear contributions [see discussion around Eqs. (1) and (2)]. The time evolution of the filament, during and after the stretching period, depends on rate and sample response (liquidlike or solidlike).

Q3: *Measurements of slip in shear-thickening fluids in the DST regime always show that the sample is solid and slipping at the tool—see, for example, the data in [72]. Given that the sample “solidifies,” in part, upon DST, is it reasonable to consider that the measurements of rheological properties after this solidification are not representative of the actual material properties?* (Norman Wagner)

A3: We fully agree that the rheological measurements after solidification (and appearance of dilatancy, slip or other flow instabilities) cannot be directly related with material properties. We, therefore, try to be very careful during these measurements and, monitoring simultaneously the response of the sample visually, determine when the sample starts to exhibit dilatancy, slip, or fracture. As discussed in the paper (as well as in the response to the first question), we relate shear and normal force fluctuations at high strains (during the start-up shear) with dilatancy and slip (see Fig. 7) and refrain from linking the normal force measured in this regime with N_1 .

TABLE I: Summary of the results obtained from the fits of the flow curve shown in Fig. 1, using, respectively, the Herschel–Bulkley equation and the three-component model with a free exponent [Eq. (1)]. Additionally, we report the viscosity of the micellar solution used as dispersing medium η_{sol} .

$\dot{\gamma}_{max}$ (s^{-1})	η_{sol} (Pa s)	Herschel–Bulkley			Three-component with free exponent			
		σ_y (Pa)	K (Pa s ⁿ)	N	σ_y (Pa)	$\dot{\gamma}_c$ (s^{-1})	η_{bg} (Pa s)	m
100	0.03	4.1 ± 0.1	2.1 ± 0.1	0.56 ± 0.01	3.4 ± 0.1	1.7 ± 0.1	0.073 ± 0.001	0.45 ± 0.01
1000	0.03	5.0 ± 0.1	1.5 ± 0.1	0.64 ± 0.01	3.6 ± 0.1	2.1 ± 0.1	0.065 ± 0.001	0.47 ± 0.01

“Pressure-driven flow and jamming of dense suspensions in channels,” Ryohei Seto and Masao Doi

We discussed a simulation model to combine lubrication flow-discrete element model (LF-DEM) and computational fluid dynamics (CFD) and demonstrated pressure-driven channel flows of monolayer particle suspensions [80]. LF-DEM [81] is a simulation model to determine particle dynamics by solving force-balance equations with frictional contacts, hydrodynamic lubrication, and other forces depending on the system to investigate. Though the simulation includes a reduced form of “effective” HIs, there is no degree of freedom for the flow; we impose a predetermined flow profile. Such a simulation with a fixed flow profile seems useful for specific situations, like rheology measurements, where the relation between velocity gradient and stress is of interest. However, LF-DEM cannot simulate conditions when flow profiles are not known a priori. To take this restriction away and investigate nonrheometric problems, we explicitly solve coarse-grained fluid dynamical equations besides force-balance equations for particle dynamics.

Q1: *What is the definition of jamming in your work and how do you characterize jammed states? Are the particles in the plug zone in isostatic conditions?* (Jin Sun)

A1: We consider jamming when velocities of particles become zero (more precisely speaking, decay exponentially). Jamming is a clogged state of particles in channels. Note that the solvent fluid can still flow or seep through clogged particles. In a jammed state, all particles achieve force balance. The force-balance equations include drag forces with local flows. Thus, the jammed state is “compatible” with only the flow which formed the structure. It is possible that some changes in the upstream can break the force-balance downstream. Plugging due to migration may be considered as a kind of jammed state. Crowds of particles are compressed, and volume fractions of compacted domains reach a maximum value. The compression may stop because the local configuration reaches a random close packing. Otherwise, the compressive stress is reduced due to a shortage of particles near walls due to migration. The suspension balance model is expected to capture this behavior.

Q2: *Have you statistically analyzed the observed force chains?* (Sarah Hormozi)

A2: In general-flow problems, statistical analysis of force chains seems more challenging than rheology simulations due to nonuniform flow conditions and wall boundaries. In dense suspension flowing through a channel, force chains develop from the sidewalls. Jamming occurs when force chains from the two sides meet at around the middle of the channel [80]. Further systematic analysis is required to obtain physical insights in such nonuniform jamming problems.

Q3: *Our experiments have shown that the fluid flow around the particle chains [73] may contribute to the progressive dilution of the suspension along the channel and to the velocity oscillations. Could you comment on whether it contributes to the relaxation of the structures in your system?* (Lucio Isa)

A3: Our simulation model incorporates fluid flows to interact with particle structures. To capture flow-particle interactions at an intermediate scale, we introduce a smoothed volume fraction field from a particle configuration. Force networks determine the rigidity/flexibility of the domain. Thus, local configurations and force networks determine the properties of the “porous media.” So far, we focus on a hard-sphere system, which has no additional time scale like shear-thickening suspensions. We are also not yet investigating yield stresses of jammed states due to a finite strength of frictional contacts. Probably, this is why we do not observe the velocity oscillations reported by Isa *et al.* [73] yet. This is one of our targets in the near future.

Q4: *Could you comment about particle migration in your work?* (Nicos Martys and Yanwei Wang)

A4: We can reproduce the migration of semidense suspensions reported in Nott and Brady’s pioneering work in 1994 [74]. Our focus is to incorporate frictional-contact forces in dense suspension with a similar setup. Nevertheless, the basic theoretical framework [74,75] almost remains intact; the normal stress imbalance causes particle migrations. Besides, we can see a dilatancy-like behavior, force chains from the boundary walls gyrate and bring particles inward.

“Modeling stress relaxation in dense, fine-particle suspensions,” Aaron S. Baumgarten and Ken Kamrin

Q1: *Could you comment on the tensorial nature of your approach and whether that could capture strain reversal?* (Itai Cohen)

A1: Our investigation of stress relaxation in fine-particle suspensions considers a special case of the fully three-dimensional model described in Baumgarten and Kamrin [76]. The stresses in this model arise from microscopic elastic deformations of individual grains and are calculated by subtracting the plastic bulk deformation rate (due to granular slip and rearrangement) from the macroscopic deformation rate. If the bulk elastic moduli (G, κ in this work) are small, the differences between the plastic and total rate may be large. This could capture some aspects of the stress changes associated with strain reversal; however, since the plasticity parameters of our model are scalars (e.g., $\varphi, f, \dot{\gamma}^p$), we cannot currently model aspects of strain reversal associated with shear band formation, granular sliding, etc. Future

work on this could focus on defining tensor forms of the fraction of frictional contacts or introduction of a fabric tensor into our plasticity model.

Q2: *The packing fraction is constant during the relaxation. Could you comment on how/if the coordination number changes?* (Farhang Radjai)

A2: The model [76] that we use in our analysis does not directly track or model the coordination number of the granular phase of the material, therefore it is difficult to comment on how it may change during the experiments we recreate. In this work, the closest scalar field we have to the coordination number is the fraction of granular interactions that are frictional in nature (f), which decreases as stress relaxes away. In future modeling efforts, the introduction of a fabric tensor model would allow us to probe this question more fully.

Q3: *Could you comment on the finite depth of the strain propagation in different conditions?* (Gareth McKinley)

A3: In the impact simulations and wheel simulations reported in Baumgarten and Kamrin [76], which use the same model studied in the present work, we observed both system spanning and transient “solidified” granular structures (associated with high fractions of frictional granular contacts). In our rod impact simulations from the former work, the “added mass” effect of the growing “solidified” region below, the impactor was enough to slow it. In the wheel simulations, on the other hand, the fast-moving wheel is observed to “climb” out of the simulated mixture much more effectively when these structures reach the bottom of the container.

Q4: *Could you comment on the difference between “relaxation” and “retardation” timescales in your modeling? Some of your flows are more akin to “stress control” (e.g., gravity-driven) where the concept of “retardation” time may be important.* (Randy Ewoldt)

A4: The “relaxation” and “retardation” timescales of the model in Baumgarten and Kamrin [76] are emergent properties and difficult to comment on without analyzing a specific geometry and flow. The analysis performed in this work focuses on how our model simplifies in the case of “relaxation” for simply-sheared samples of corn starch-water mixture subject to sudden arrest, but we have not performed a similar analysis for “retardation” problems. This is certainly an interesting area to look at in the future but is difficult to comment on now.

Q5: *How many fitting parameters do you need to reproduce reliable results?* (Hisao Hayakawa)

A5: The model we analyze in this work is from Baumgarten and Kamrin [76] and has 19 total fitting parameters. Many of these parameters have some physical description (e.g., maximum packing fraction at which steady flow is possible, repose angle of the granular material, fluid viscosity, etc.) and all but the four analyzed in this work (K_0 , K_4 , G , and κ) can be reliably determined from the fitting procedures described [77] and the supplemental material of [76].

Q6: *Are the particle size and fluid viscosity effects captured in your “corn starch” mixture model?* (Yoel Forterre)

A6: In our “complete” corn starch model found in the supplemental information from Baumgarten and Kamrin [76], we do account for the Darcy law drag arising from independent motion of the fluid and solid parts of the corn starch-

water mixture. Indeed, this drag relation calls upon the grain size. For the simplified analysis reported in this work we have assumed that the mixtures are comoving, but in the simulations shown previously [76], we use the full model (including Darcy drag).

Q7: *Have you simulated corn starch in a parallel-plate rheometer? If so, do you see the pressure heterogeneities found as described in the talk by Gauthier et al. [68]?* (Jeffrey Urbach)

A7: We have not simulated corn starch in a parallel-plate rheometer, so we cannot comment. It would be interesting in the future to examine this problem and see if these heterogeneities arise.

Q8: *How is the stress relaxation here (due to relaxation of particle network) different from Brownian stresses?* (Vikram Rathee)

A8: The stress relaxation modeled in this work arises due to grain slip after cessation of macroscopic flow coupled with decay in the particle network (modeled here by f). This decay rate is described in Baumgarten and Kamrin [76] and is associated with four primary modes of change: (1) growth in shear as grains are pushed together, (2) decay in shear as grains slip past each other, (3) decay due to microscopic force chain breakdown, and (4) decay due to Brownian motion. In our work, we have generally considered this fourth term to be negligible in comparison to the other three and have not investigated it further. It would be interesting in the future to try to model this type of decay and see how it interacts with the other mechanisms in our model.

“Constitutive model for shear-thickening suspensions: Predictions for steady shear with superposed transverse oscillations,” Jurriaan J. J. Gillissen, Christopher Ness, Joseph D. Peterson, Helen J. Wilson, and Michael E. Cates

Q1: *In a very densely packed system, i.e., for high coordination number Z , the anisotropy cannot be too high. Hence there is a coupling between the trace and the deviatoric part of the fabric tensor. Have you considered that in your model?* (Farhang Radjai and Bulbul Chakraborty)

A1: Our microstructure tensor evolution equation [Eq. (24) of the paper] is equivalent to six coupled partial differential equations for six scalars, i.e., the time evolution of each tensor component depends on the values of all the tensor components. Equivalently, the time evolution of the trace of the tensor depends on the deviatoric part of the tensor and vice versa.

Q2: *The model assumes two-body lubrication analysis, even the distribution function is based on the Smoluchowski equation for the two-particle configuration space. How valid is this assumption for dense suspensions where many-body effects are prominent?* (Tabish Khan)

A2: Truncating the statistical description at the pair level provides sufficient information to capture qualitatively rheological behavior that is observed in experiments and simulations, e.g., normal stress differences, transient stresses after shear reversal, shear thickening and oscillation thinning. Clearly, however, collective phenomena are important in principle, and may be responsible for some of the

quantitative discrepancies with experiment and simulation data that we have reported. Less clear is precisely how to include these phenomena within a manageable mathematical framework.

Q3: *Is this constitutive model inspired from the liquid crystal theory? If so, can you please discuss the similarities and differences between the proposed model and the constitutive equation for liquid crystals?*

A3: Our microstructure is based on particle pairs and these pairs rotate as rods (which is similar to liquid crystals). In addition, these pairs are being created and destroyed when two particles move toward and away from each other (which differs from liquid crystals).

The next four questions are answered together.

Q4: *The model predicts viscosity reduction with oscillations in the unthickened state, which to my knowledge is not observed in the simulations. Could you comment on this?* (Romain Mari)

Q5: *What happens to the model if we reduce to the isotropic case, where $\langle nn \rangle = I/3$?, i.e., how important is the anisotropy?* (Mehdi Pouragha)

Q6: *Why is it that for all shear rates, the orthogonal oscillatory shear rate of 1 results in diminishing of shear-thickening behavior?* (Reza Foudazi)

Q7: *Can your model capture the observed higher shear jamming packing fractions at large shear oscillations?* (Martin Trulsson)

A4–7: For low shear rates (unthickened state), the suspension viscosity is dominated by lubrication films. For large shear rates (thickened state), the suspension viscosity is dominated by direct particle contacts. As we apply low amplitude orthogonal oscillations to a sheared suspension, then the microstructure becomes more isotropic. For low shear rates, this isotropization results in thicker lubrication films. For high shear rates this tendency toward isotropy results in reduced particle contacts. Both thicker films as well as reduced contacts reduce the suspension viscosity. The reduced contacts (at a given volume fraction) also increase the jamming volume fraction, at which point the number of contacts reaches its critical value.

Q8: *The separation into E and E_c is a great idea. However, unlike the usual symmetric E , E_c is not straightforward to calculate and requires diagonalization of the local strain rate tensor. If this is implemented in a complex flow (in a numerical flow solver), what should one do to calculate E_c ?* (Peter Olmsted)

A8: Indeed, our solver diagonalizes the rate of strain tensor to find its eigenvectors, which represents a dominant part of the overall numerical workload when addressing non-uniform flows.

“Unifying viscous and inertial regimes of discontinuous shear-thickening suspensions,” Junhao Dong and Martin Trulsson

Q1: *Is granular stress the same as inertial stress in your work?* (Bloen Metzger)

A1: Indeed, by granular stress we refer to inertial stress. When discussing granular stresses, we had actually in mind a dry granular matter, which is dominated by inertial

stresses. A bit sloppy in terminology, we used inertial and granular stresses interchangeably in our paper [see Eqs. (9) and (10)].

Q2: *Due to adhesion and other factors, the friction coefficient usually drops with load, and it may be more appropriate to use a constant frictional force rather than friction proportional to load in many cases. Have you considered that?* (Mark Robbins)

A2: We did in fact test a model where the friction coefficient decreased with the normal load, similar to what is proposed, see Fig. 10 in our paper. In Fig. 10(b) one can see that this, under certain circumstances, can lead to a double cusp (i.e., alternating between a positive and a negative compressibility). Our model of the friction coefficient is, however, phenomenological and developing more realistic models would be an interesting idea to pursue.

Q3: *In Fig. 8(a) of the paper, all the curves representing different protocols cross a single point. Could you comment about that the significance of the crosspoint?* (Omer Sedes)

A3: Yes, all curves cross at one point. This was by construction. As it turns out, it was easier (visually) to see the effect of various shear protocols if they shared a common point. The curves could have equally gone through any other point (by specifying another parameter couple: ϵ and K_0). Our point in Fig. 8(a) of our paper corresponds to $\epsilon = 1$ and $K_0 = 2e^{-4}$. The same value of K_0 was used in Fig. 8(b).

Q4: *Could you comment about the relative ratio of the viscous to the inertial viscosities as a function of the volume fraction?* (Romain Mari and Jeff Morris)

A4: Relating the viscosity to the various dissipation mechanisms, the relative importance between viscous and inertial dissipations seems to be controlled by the I/J ratio [78] (essentially a rescaled pressure). See our paper and [78,79] for definitions of I and J . As one approaches shear jamming at a fixed Stokes number the ratio changes, leading to the conclusion that inertial dissipation dominates close to shear jamming (see Fig. 7 of [1]). This prediction is based on the assumption that the viscous and inertial dissipations can be linearly added. Numerical support for this can be found in Fig. 1 of [78]. The data points in the same figure were, however, successfully fitted to a simple expression involving the Stokes number ($St = I^2/J$ in our formulation), supporting the idea that St controls the relative importance, i.e., the relative importance does not change when approaching shear jamming at a fixed Stokes number. Inferring the relative importance instead from the macroscopic friction coefficient supports the idea that the relative importance is given by St (see our paper and [78]). This measure might, however, be too imprecise to disentangle the relative importance close to shear jamming as both viscous and inertial particle flows have the same critical friction coefficients at shear jamming. Since the linearity (of the dissipation mechanisms) was never tested numerically in [79] (i.e., simulations with both inertial and viscous contributions) and only one packing fraction was tested in [78] (and with one tested expression), this question (i.e., if St or I/J gives the relative important of the various dissipation mechanisms approaching shear jamming) should, in our view, be regarded as partly unresolved.

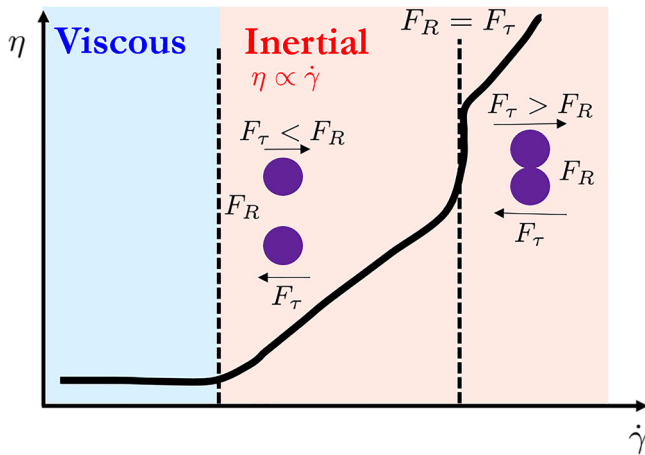


FIG. 3. Inertial shear thickening in the presence of friction can eventually give way to discontinuous shear thickening (DST). Here, F_R is a repulsive interparticle force, while F_τ is a force due to shear flow, and viscous-inertial thickening occurs at lower rate than DST. Styled after Fig. 3 of [43].

“Shear thickening in dense non-Brownian suspensions: Viscous to inertial transition,”

Q1: Do you use a single Stokes number or the Stokes and Reynolds numbers to quantify inertia? (Chaithanya K. V. S.)

A1: Our suspension is density matched. Therefore, the Stokes number and particle Reynolds number are identical up to a constant numerical factor.

Q2: Could you clarify the salt concentration and if the amount of salt can affect the results? (Mark Robbins and Abhinendra Singh)

A2: We did not perform AFM with varying salt concentrations. The amount of salt was determined to have a density-matched suspension. We presume that the repulsive forces will be lower if we increase the salt in the solvent. To shed some light on this, the group of Annie Colin will publish a paper on the AFM measurements for various solvents in the near future.

Q3: The transition from viscous to inertial is found at very high-volume fraction (0.595, with the jamming point reported at 0.605). Could you comment on the absence (or presence) of DST (discontinuous shear thickening) in your system? Are lubrication forces too strong to let particles coming into contact? (Tabish Khan)

A3: We study the Bagnoldian mode of shear thickening and not DST. Our AFM measurements show that the repulsive forces are strong enough to prevent contact. Therefore, in our system, DST may occur at much larger shear rates. The cartoon of Fig. 3 better clarifies our system of study. The schematic shows a short-range repulsive force (F_R) among the grains preventing contact formation. As we increase the shear rate, normal stresses between the grains due to the shearing motion (F_τ) will overcome the repulsive forces (at a shear rate higher than that of viscous to inertial transition), converting the system into an assembly of frictional grains with a viscosity that changes abruptly. In this work, our investigation is limited to the viscous to inertial transition in dense non-Brownian suspensions in the absence of friction (Fig. 3).

“Permanent shear localization in dense disordered materials due to microscopic inertia,” Kirsten Martens

This talk was associated with [24].

Q1: Could you comment on how the dimensions perpendicular to the gradient direction, which are relatively small, may have any effect on the persistence of shear bands? (Mark Robbins and Ishan Srivastava)

A1: Indeed in situations where the shear rate range asks for a large gradient dimension to allow the instability to develop, we are using very particular box dimensions to be able to handle the computation time needed to achieve a stationary state. The ratio between the simulation length in the shear direction and in the gradient direction is in that case indeed very small and we are thus simulating effectively a quasi-one-dimensional system. So this question is very relevant to our study. One could think that our one-dimensional theory only works well for predicting the onset of the instability because we designed the simulation study in a way that will confirm it.

To address that question and to test the predictability for the onset of the instability in three dimensions, we also performed simulations on systems with a much larger aspect ratio, namely, $360 \times 80 \times 80$ in units of the average particle diameter, but still with the large length in the gradient direction. With this more reasonable ratio, we still find a good agreement for the onset of the instability between the theory and simulations, which makes us more confident concerning the quasi-one-dimensional character of the problem as long as we are dealing with bulk dynamics and a bulk dissipation mechanism. But of course it will be interesting to go beyond this simplified setup and study the dynamics of truly three-dimensional systems, especially when dealing with wall effects, and particularly if dissipation is a wall-dominated process.

“The role of friction in the yielding of adhesive non-Brownian suspensions,” J. A. Richards, B. M. Guy, E. Blanco, M. Hermes, G. Poy, and Wilson C. K. Poon

Q1: What are the origins of different forces considered and over which range of distances would they typically operate? (Itai Cohen)

A1: Our model relies on the range of the adhesive interactions normalized to the particle size being smaller than the strain needed to push particles into frictional contact upon shear reversal. For the data shown in Fig. 4 of the paper, this strain is of order 0.1 and this sets an upper bound on the adhesive range. Beyond that and as with the Wyart–Cates model, we cannot determine the microphysical origins of forces from the rheology alone and we rely on Wittgenstein’s dictum: “that whereof we cannot speak, thereof we must remain silent.”

Q2: Can we think of the adhesive interactions you discuss as introducing additional constraints with respect to sliding friction, such as rolling friction? If yes, would these constraints operate in different conditions from those that would lead to the emergence of the yield stress? One may argue that the constraints come into play only once particles are in close contact, whereas the yield stress would emerge from large scale structural organization at relatively low stresses. (Heinrich Jaeger)

A2: Absolutely. The key to our paper is that adhesive interactions constrain rolling. Taking friction and adhesion together, there are a number of possibilities, depending on surface details. Consider, e.g., sterically stabilized PMMA in hydrocarbon solvents. When the stress reaches some

threshold, σ^* , the stabilizing “hairs” collapse and particle surfaces come into contact. In principle, this turns on both friction and adhesion, the latter of strength σ_a . What happens next depends on σ^*/σ_a . If $\sigma^* > \sigma_a$, then the flow thereafter only has sliding constraints and no rolling constraints. On the other hand, if $\sigma^* < \sigma_a$, then the subsequent flow will have sliding and rolling constraints until the stress has further increased to beyond σ_a . Now, for “bare” particles like the corn starch in oil studied in our paper, we imagine that there is nothing stopping the particles contacting right from the start, both frictionally and adhesively. Only strain is required to form such contacts and deformation will have inevitably happened in the sample history. As stress increases, the sliding constraints due to friction remain, but the rolling constraints due to adhesion are progressively broken and the suspension yields.

Q3: *What is the contribution of the surfactants to the yield stress? Is there a scaling prediction for how they can modify yield stress?* (Randy Ewoldt)

A3: In the corn starch-in-oil system presented in this paper no surfactants are added and the impact of friction was studied through varying rheological protocols, comparing steady, oscillatory and reversal flows. Related studies [80,81] suggest monolayer coverage of a surfactant is key to reducing the yield stress of non-Brownian suspensions. However, the mechanism of impact for the surfactant depends on chemical details. In a model sugar-in-oil suspension, the phospholipid lecithin reduces the friction coefficient between particles, lowering the yield stress by increasing the high-stress jamming volume fraction. In contrast, poly-glycerol–poly-ricinoleate and poly-(acrylic acid) in an aqueous calcite suspension both introduce separation (repulsion) between particles. While this reduces adhesion it also crucially prevents frictional contact below a critical stress, above which they are displaced from the surface. By preventing frictional contact at low stress such surfactants dramatically lower and practically eliminate the yield stress. Further addition of surfactants beyond apparent monolayer coverage does not increase their impact. In the case of lecithin, further addition is deleterious, possibly inducing attraction between particles; however, a detailed investigation of the scaling before this point has not been performed.

Q4: *If imposed to a steady-state shearing, an elastic material does not flow, and instead stretches elastically. Hence, if determined from the flow curve, the yield stress identified could be rather a dynamic yield stress whereas a better insight into sticky interactions may come from a static yield stress, that you could measure, from the height of a stress overshoot in a start-up shear experiment. How do you determine that the system is flowing when measuring yield stress?* (Simon Rogers and George Petekidis)

A4: We absolutely agree with the claim that the yield stress measured depends on protocol, which is the main message of Fig. 3 in our paper. The static yield stress is likely to be higher than even our flow yield stress. However, we have not explored the static yield stress in detail because its value may be time dependent. As in many systems, the longer we leave a sample quiescent, the higher the static yield stress is likely to become, whereas for the three protocols that give the data in Fig. 3, time-dependent effects do not control the result.

Q5: *Are the suspensions you are working with thixotropic?* (Jim Swan)

A5: Perhaps, but we have not explored it. (See also our answer to the above question from Petekidis and Rogers.)

“Rheology of visco-cohesive granular flows,” Farhang Radjai, Thanh Trung Vo, Saeid Nezamabadi, Patrick Mutabaruka, and Jean-Yves Delenne

This presentation was associated with [26].

Q1: *How do your inertial dimensionless numbers compare to others used in the literature?* (Itai Cohen)

A1: We introduced a “viscoinertial” dimensionless number in Amarsid *et al.* [82] for 2D sheared suspensions simulated by means of a coupled DEM-LBM method. For different values of the fluid viscosity, shear rate, density ratio, and confining pressure (exerted only on the granular phase), the effective friction coefficient and packing fraction appear to be unique functions of this viscoinertial number. We also showed that the same number scales also the texture variables (coordination number and fabric anisotropy). This number is similar (although formulated differently) to that introduced by Trulsson *et al.* [78] for their DEM simulations without suspending fluid but involving viscous drag force applied directly on the particle centers in sheared packings. Recently, we performed extensive simulations in 3D by including both viscous drag forces and cohesive forces between grains. Based on previous work, we extended the viscoinertial number to include the cohesion index (the ratio of cohesive stress between particles to the confining stress). We find that by varying various parameters, the effective friction coefficient and packing fraction, normalized by their values in the quasistatic state, can each be expressed as a unique function of this cohesive viscoinertial number. This has, so far, no experimental counterpart, and we are aware of no other work mentioning a similar result or scaling parameter for inertial cohesive granular materials. It would be highly interesting to compare with independent numerical or experimental work on the subject. It should be noted that the cohesive viscoinertial number is equal to the inertial number for dry cohesionless granular media, to the viscous number of Boyer *et al.* [57] in the limit of low inertia and no cohesion, to the viscoinertial number in the limit of no cohesion. In this sense, it includes all the other dimensionless numbers introduced previously.

Q2: *How do different microscopic length scales affect your analysis of the rheology?* (Ishan Srivastava and Abhinendra Singh)

A2: The simulated system in our recent work involves three length scales: particle diameter, debonding distance of the capillary bridges between particles, and a cutoff on the lubrication force. The particle diameter naturally enters the cohesive viscoinertial number as it does for the inertial number. The two other lengths do not affect the general expression of the cohesive viscoinertial number, but they are expected to influence the values of the two free parameters in this general expression. We did not check this point, and further work is needed to confirm. The same remark applies to all other material parameters such as particle shape and friction coefficient. We expect the two free parameters of the dimensionless number to depend on such parameters.

“On the viscosity of adhesive hard sphere dispersions,”

James Swan

This was associated with [27].

Q1: *In your simulations, is twisting around the bond that connects to particles allowed? Could you comment about the differences or similarities with simulations for grains that implement both sliding and rolling friction?* (Wilson Poon)

No. In these simulations, we constrain all relative motion including rolling and twisting. In this work, the friction coefficient is essentially infinite for all the modes of relative motion between particles. We could relax the constraint on twisting without difficulty and this may play a role in determining the conditions under which the viscosity diverges.

Q2: *Could you comment on how the lubrication forces depend on the small and on the larger radius of the raspberry particles?* (Nicos Martys)

These simulations have no explicit lubrication interactions incorporated into them. The short-ranged hydrodynamics emerge from the boundary element calculations. We have estimated the deviation from predictions of exact solutions of the Stokes equations between particle pairs and errors smaller than 10% in the forces on nearly touching particles are expected until the particles get within about half a bead radius of one another. However, in these simulations, we constrain such particles to have no relative motion. With no relative motion, there is no diverging lubrication force and the simulations retain their high level of accuracy.

Q3: *Could you comment on possible ordering induced by the boundaries?* (Shivakumar Athani)

In these simulations, periodic boundary conditions are employed. We see no signs of boundary induced ordering.

“Formation of stable aggregates by fluid-assembled solid bridges,” Ali Seiphoori, Xiao-guang Ma, Paulo E. Arratia, and Douglas J. Jerolmack

This talk was associated with [28].

Q1: *Could you clarify the range of volume fractions for different size ratios?* (Itai Cohen and Vikram Rathee)

A1: Volume fractions are all indicated in the paper.

Q2: *If you add up all the surface area of the tiny particles, is that so much larger than the surface area of the other particles that that is the reason why the size dominates over the chemistry? Or is there some scaling law for the interactions that can be identified? If we think that clay particles are mainly platelets, how can we make sense of the role of tiny particles in between the platelets?* (Heinrich Jaeger and Karen Daniels)

A2: We think that, in the end, it is all about surface area. This is the primary reason why different materials are all cohesive when they include particles smaller than 5 μm and are not cohesive when particles $<5 \mu\text{m}$ are excluded. We rationalize this through calculations of the relevant forces, showing that when interparticle forces exceed particle weight then the effective cohesion becomes relevant (see SI Appendix, Fig. S6).

Q3: *Could you comment on the ion concentration in the solutions (which could even be introduced by the natural particles)? The concentration could increase by several orders of magnitude during evaporation, which would decrease the electrostatic repulsion of the particles quite a lot.* (Lars Kool)

A3: Good question. We used de-ionized water and so did not introduce ions intentionally. We do not know if/how the ionic strength may have been altered by introducing particles themselves.

Q4: *How “dry” is your system? Could you comment about the fluid bridges that remain in your system upon drying and how drying may change adhesion? Could you also comment on what are the specific mechanisms to entrain fluid (seemingly within the boundary layer) to magnify the capillary effect? Recent work in the adhesives community exploits physical adhesion through capillary forces and identifies particle anisotropy as a key factor, so I ask whether your work points to anisotropy in distribution (through hierarchy) as meaningful as well.* (Ruel McKenzie)

A4: After evaporation, there is still likely to be water present and associated adhesion; the suspensions were evaporated under ambient room conditions. However, the deposited aggregates then experience plasma cleaning that we perform for the slide they are on so that we can mount the microfluidic chamber. In other words, the rewetting experiments that probe the stability of aggregates are conducted on very dry aggregates. We did not explicitly explore anisotropy effects; surely the clay particles have anisotropic effects that matter, but this is beyond the scope of the current study. We examined only size effects.

Q4: *Could you comment on the hierarchy of lengthscales, how separated they need to be and how polydispersity plays a role in this?* (Chinedum Osuji)

A4: Great question. We really do not know. Our particles were different by factors of at least 5 and typically an order of magnitude. I do not know whether the segregation would persist if the particles were “only” a factor of 2, or 2.5, different.

Q5: *Could you comment on the role of the colloid-substrate interactions and how is that substrate dependent?* (Ramya Koduvayur)

A5: We did not explore substrate controls very much. We used borosilicate glass coverslips that were negatively charged, like the particles deposited on them. We did explore the effects of making the surface more hydrophilic; in particular, we treated the surface with O_2 plasma that ensured that the droplet was not “pinned” to the substrate—this allowed particles to be pulled inward to make a single large aggregate. We performed experiments without that treatment, and results were qualitatively similar; but, the pinning of the droplet made it break up into smaller droplets as it evaporated, and this led to smaller and more numerous aggregates dispersed on the slide.

“Variations of the Herschel–Bulkeley exponent reflecting contributions of the viscous continuous phase to the shear rate-dependent stress of soft glassy materials,” Marco Caggioni, Veronique Trappe, and Patrick T. Spicer

Q1: *Have you observed any edge fracture at higher shear rates for experiments done in a rotational rheometer?* (Yogesh Joshi)

A1: We explored the flow behavior of our emulsions using a cone and plate geometry ($\leq 100/\text{s}^{-1}$) and a Couette geometry ($\leq 1000/\text{s}^{-1}$). Within these shear rate ranges, we did not observe edge fracture in either geometry and the results obtained in both geometries were essentially identical within the common shear rate ranges.

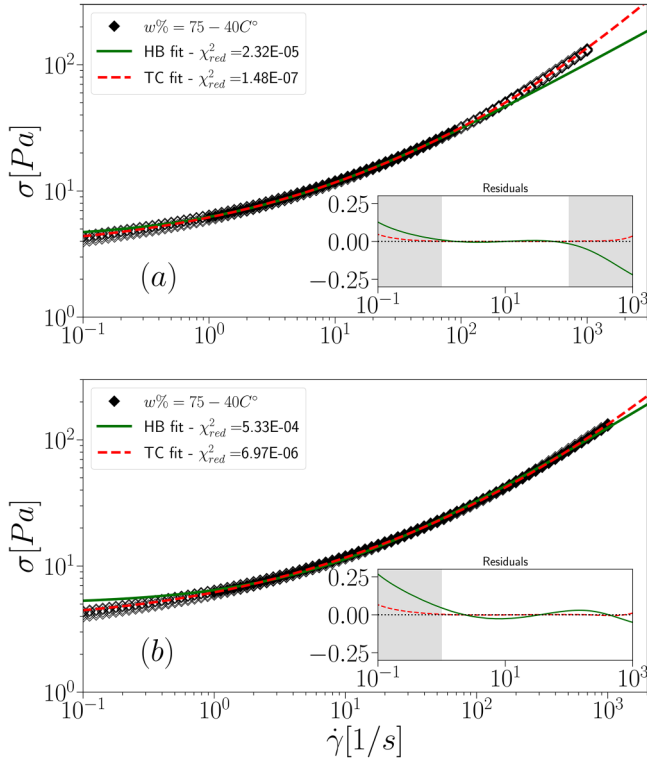


FIG. 4. Flow curve obtained at 40 °C for 75 wt. % oil in LAS emulsion. The analysis shown is equivalent to that shown in Fig. 3 of the paper, except that we here leave the exponent of the second term in the three-component model to be a fit parameter [see Eq. (1)]. Solid green lines denote the best fits of the data to the Herschel–Bulkley model; the dashed red lines denote the best fits to the three-component model. (a) The data used for the fits are limited to 1–100 1/s⁻¹. (b) The data used for the fits are limited 1–1000 1/s⁻¹. Insets: residuals expressed as relative deviation of the fit values from the true values; solid green lines correspond to the residuals obtained with the Herschel–Bulkley-fits and the dashed red lines to those obtained with the three-component-fits. The shaded range indicate the range of extrapolated fit values.

Q2: *Could you comment on the error bar on the exponent in the power law and how that may change (from 1/2 to 2/3) once you add the third component?* (Mark Robbins)

A2: To answer whether the exponent of the second term in Eq. (4) of the paper could be 2/3 instead of 1/2, we performed an analysis similar to that shown in Fig. 3 of the paper, using a three-component model with a free exponent m in the second term

$$\sigma = \sigma_y + \sigma_y \cdot \left(\frac{\dot{\gamma}}{\dot{\gamma}_c} \right)^m + \eta_{bg} \cdot \dot{\gamma}, \quad (1)$$

and restricting the data range used for the fit to, respectively, $\dot{\gamma} = 1 - 100$ 1/s⁻¹ and $\dot{\gamma} = 1 - 1000$ 1/s⁻¹, as shown in Figs. 4(a) and 4(b). As for the original three-component model, a fit based on Eq. (1) delivers a better description of the data outside the range used for the fit than the Herschel–Bulkley model. The resulting exponent m tends to be somewhat smaller than 1/2, as shown in Table I. For the flow behavior of emulsions, $m = 1/2$ seems therefore to be the better descriptor than $m = 2/3$.

Q3: *For deformable particles one would expect dissipation due to deformation to introduce another timescale, while at high enough rates the time-dependent deformation will be either nonexistent or settle into a specific shape. Therefore, two high shear rate limits could be observed: one with a sub-Newtonian exponent controlled by the particle deformation, and a final Newtonian relation. Could you comment on this and whether it can give a 2/3 exponent for the power law in the crossover regime?* (Peter Olmsted)

A3: Adding a fourth term to Eq. (4) of the paper would certainly be feasible. However, based on the analysis with Eq. (1) the range over which a power of 2/3 would apply would be very small and difficult to capture properly. With the three-component model as it stands, we accounted only for three regimes, which we denoted as elastic, plastic and viscous dissipation regimes. Additional dissipation mechanisms may have to be considered. Let us here emphasize that the point we most wanted to make is that the Herschel–Bulkley model has no physical meaning associated with at least two of its three parameters. In particular, the Herschel–Bulkley exponent should not be regarded as a physical parameter worth interpreting, as it mainly reflects the range of high shear rates probed in an experiment. By introducing equations with terms that can be clearly associated with dissipation mechanisms, we believe more progress can be made in our understanding of the flow behavior of yield stress fluids in future work.

Q4: *Can you comment on how/if one can link the parameters of the three-component model to intrinsic properties of the suspension?* (Chinedum Osuji)

A4: As pointed out in the paper, we believe that the main advantage of the three-component model over the Herschel–Bulkley model is the possibility of a direct connection of the model parameters with material properties. The model incorporates the dynamic yield stress, σ_y , the onset of plastic dissipation at the critical shear rate, $\dot{\gamma}_c$, and the terminal viscosity at high shear rates, η_{bg} . For a concentrated emulsion, the yield stress is controlled by a number of parameters including the volume fraction of dispersed phase, the size, and the interfacial tension of the dispersed droplets. Testing the parameters that govern $\dot{\gamma}_c$ and η_{bg} in dense packings is actually the next step, we need to undertake to progress. As noted by Peter Olmsted in Q3, one of the material properties likely to be important is the deformability of the emulsion droplets as well as the viscosity of the continuous phase.

“Pipe flow of sphere suspensions having a power-law-dependent fluid matrix,” Nicos S. Martys, William L. George, Ryan P. Murphy, and Kathleen M. Weigandt

Q1: *Could you comment on finite size effects in your study?*

A1: We did not do a detailed study of finite size effects. The ratio of the diameter of the solid inclusions to the pipe diameter was approximately 1/30. So, it would be expected, although not proven, that the general flow characteristics would be insensitive to decreasing this ratio. The reason we chose this ratio was that it is similar to that of sand in a mortar flowing through a nozzle used for 3D printing. If this ratio increased, we would expect to see some evidence of finite size effects as it approaches 1.

Q2: *Have you observed any evidence of particle layering?*

A2: While we saw evidence of ordering as the volume fraction increased, it was difficult to directly see a layering effect, although there may be a hint of this at the highest volume fractions studied. In general, this type of effect might have been limited due to the modeling of flow in a cylindrical pipe. It is more likely a layering effect would be seen in a rectangular channel or perhaps when the pipe diameter is much greater than the inclusion diameter such that the pipe wall appears as a flat surface to the inclusion.

Q3: *How did you take averages of the radial flow field?* (Sarah Hormozi)

A3: To determine the average radial flow field of the inclusions a set of 8–10 equally spaced concentric bins were constructed that extended from the pipe axis of symmetry to the pipe wall. The average velocity of the solid inclusions whose center fell in a bin was determined and plotted with respect to the center of each bin.

Q4: *Can this type of study also cover converging channels and which aspects of those flow can be elucidated?* (Ruel MaKenzie)

A4: Yes. The approach used in our simulations could be adopted for modeling flow through converging channels and other complex geometries. Although we have not modeled converging channels, we have modeled suspension flow in coaxial rheometers with a vane or spiral impeller. Such studies have provided physical insight into the interpretation of experimental measurements as the complex flows that develop in such devices are not amenable to analytic solution and exhibit many flow artifacts.

“Excess entropy scaling for soft particle glasses,”
Roger T. Bonnecaze, Fardin Khabaz, Lavanya Mohan, and Michel Cloitre

Q1: *How do you rationalize the value of excess entropy you find? Can it be connected to specific microstructural features?* (Poornima Padmanabhan)

A1: The excess entropy can be interpreted as a measure of free volume or relative freedom of movement of the particle apart from the shear. These are greater with increasing excess entropy. The excess entropy is determined by the distribution of particles. In this paper, we used the two-body contribution in Eq. (6) to approximate the excess entropy, which is determined from the particle pair-distribution function.

Q2: *Could corrections beyond pairwise interactions (three- and higher-order corrections) to the excess entropy be non-negligible?* (Jerry Wang)

A2: Indeed, there are corrections to the excess entropy beyond pairwise interactions. See, for example, Baranyai and Evans [83], where the excess entropy is expressed in two-body, three-body, and higher-order corrections. Higher-order corrections could be non-negligible and that is perhaps one explanation for why the excess entropy does not work as well at the lowest volume fraction of 0.7.

Q3: *Could you comment about the linear response regime in systems with different yield stresses? Is it possible to rescale the response in the linear regime in the same manner as for the nonlinear?* (Simon Rogers)

A3: We have found in several of our studies on soft particle glasses that many parameters (e.g., normalized shear and normal stress and shear-induced diffusivity of particles) can be correlated and collapsed onto universal curves using $\eta\dot{\gamma}/G_0$, where η is the viscosity of the suspending fluid, $\dot{\gamma}$ is the shear rate, and G_0 is the low-frequency shear modulus. The volume fraction dependence is captured by the shear modulus. In a study being prepared for submission, we have found this rescaling works well in the linear regime of small amplitude oscillation (e.g., for storage and loss modulus), where the shear rate is replaced by the frequency.

Q4: *Does the softness of the particles change the excess entropy and would these ideas apply to hard particles such as silica?* (Abhinendra Singh and Itai Cohen)

A4: The softness does affect the excess entropy. The effect is shown in Fig. 4, where the excess entropy is a function of shear rate nondimensionalized with either the modulus of the particle [Fig. 4(a)] or the shear modulus of the suspension [Fig. 4(b)]. At a given shear rate, the excess entropy is greater the softer the particle is. Certainly, the excess entropy can be computed for suspensions of hard particles. For example, it can be estimated with the two-body approximation for excess entropy using the pair-distribution function in Eq. (6).

Q5: *How does your analysis correlate with the concept of granular temperature?* (Farhang Radjai)

A5: Granular temperature is the root mean square of grain velocity fluctuations. This is related to the particle diffusivity, which can be expressed as the autocorrelation of the velocity correlations or the product of the square of the velocity fluctuations and correlation time. Certainly, the diffusivity can be correlated to excess entropy [Fig. 7(a)] and through Eq. (7) to stress and through the correlation in Fig. 6 to the temperature. The correlation time has been computed [14] and correlated with the excess entropy. Putting it all together, the granular temperature can be related to the temperature defined in this paper.

Q6: *In certain cases, as you reduce volume fraction, your results deviate from the proposed scaling (see, for example, volume fraction of 0.7). Is there a physical reason for this?* (Ruel McKenzie)

A6: It is not clear what is causing the deviations in the entropy scaling for diffusivity and stresses at the volume fraction of 0.7. It could be that the two-body approximation for excess entropy [Eq. (6)] is not accurate enough. It could also be that the entropy scaling is not correct at the lowest volume fraction.

Q7: *Could you comment on the magnitude of N_2 with respect to N_1 , with respect to other physical systems (see, for example, atomic fluids or high pressure fluids)?* (Mark Robbins)

A7: For these soft particle glasses, the second normal stress difference is about the same magnitude as the first normal stress difference but of an opposite sign. Essentially, the normal stress component in the velocity gradient direction dominates the other normal stresses giving this behavior. Ron Larson has shown [84] that so-called film-fluids, where the elastic forces generated are due to deformations to the surfaces of the particles in the suspension, have normal

stresses that are about equal in magnitude and opposite in sign as observed in our work.

ACKNOWLEDGMENTS

Much of this work benefited from the KITP program “Physics of Dense Suspensions” January–April 2018; research associated with this program was supported in part by the National Science Foundation under Grant No. NSF PHY-1748958. JFM was supported by Grant No. NSF 1916879.

REFERENCES

- [1] Del Gado, E. D., and J. F. Morris, “Preface: Physics of dense suspensions,” *J. Rheol.* **64**(2), 223–225 (2020).
- [2] Ong, E. Y. X., M. Ramaswamy, R. Niu, N. Y. C. Lin, A. Shetty, R. N. Zia, G. H. McKinley, and I. Cohen, “Stress decomposition in LAOS of dense colloidal suspensions,” *J. Rheol.* **64**(2), 343–351 (2020).
- [3] Hsu, C.-P., S. N. Ramakrishna, M. Zanini, N. D. Spencer, and I. Lucio, “Roughness-dependent tribology effects on discontinuous shear thickening,” *Proc. Natl. Acad. Sci. U. S. A.* **115**(20), 5117–5122 (2018).
- [4] Clavaud, C., B. Metzger, and Y. Forterre, “The Darcytron: A pressure-imposed device to probe the frictional transition in shear-thickening suspensions,” *J. Rheol.* **64**(2), 395–403 (2020).
- [5] Lee, Y.-F., Y. Luo, S. C. Brown, and N. J. Wagner, “Experimental test of a frictional contact model for shear thickening in concentrated colloidal suspensions,” *J. Rheol.* **64**(2), 267–282 (2020).
- [6] Singh, A., C. Ness, R. Seto, J. J. de Pablo, and H. M. Jaeger, “Shear thickening and jamming of dense suspensions: The ‘roll’ of friction,” *Phys. Rev. Lett.* **124**(24), 248005 (2020).
- [7] Bourriane, P., V. Niggel, G. Polly, T. Divoux, and G.H. McKinley, “Unifying disparate experimental views on shear-thickening suspensions,” [arXiv:2001.02290](https://arxiv.org/abs/2001.02290) (2020).
- [8] Wang, M., S. Jamali, and J. F. Brady, “A hydrodynamic model for discontinuous shear-thickening in dense suspensions,” *J. Rheol.* **64**(2), 379–394 (2020).
- [9] More, R. V., and A. M. Ardekani, “Roughness induced shear thickening in frictional non-Brownian suspensions: A numerical study,” *J. Rheol.* **64**(2), 283–297 (2020).
- [10] Sedes, O., A. Singh, and J. F. Morris, “Fluctuations at the onset of discontinuous shear thickening in a suspension,” *J. Rheol.* **64**(2), 309–319 (2020).
- [11] Rathee, V., D. L. Blair, and J. S. Urbach, “Localized transient jamming in discontinuous shear thickening,” *J. Rheol.* **64**(2), 299–308 (2020).
- [12] Thomas, J. E., A. Goyal, D. S. Bedi, A. Singh, E. Del Gado, and B. Chakraborty, “Investigating the nature of discontinuous shear thickening: Beyond a mean-field description,” *J. Rheol.* **64**(2), 329–341 (2020).
- [13] Xu, Q., A. Singh, and H. M. Jaeger, “Stress fluctuations and shear thickening in dense granular suspensions,” *J. Rheol.* **64**(2), 321–328 (2020).
- [14] Khabaz, F., M. Cloitre, and R. T. Bonnecaze, “Particle dynamics predicts shear rheology of soft particle glasses,” *J. Rheol.* **64**(2), 459–468 (2020).
- [15] Pradeep, S., A.R. Jacob, and L.C. Hsiao, “Jamming distance dictates colloidal shear thickening,” [arXiv:2007.01825](https://arxiv.org/abs/2007.01825) (2020).
- [16] Barcelos, E., S. Khani, A. Lee, J. Peet, and J. Maia, “Rheology and structure of dense colloidal suspensions in confined flow,” presented at the Virtual Symposium on the Physics of Dense Suspensions, July 9–10, 2020.
- [17] H. Hayakawa, “Impact-induced hardening on dense frictional suspensions,” [arXiv:2005.02719v4](https://arxiv.org/abs/2005.02719v4) (2020).
- [18] Andrade, R. J. E., A. R. Jacob, F. J. Galindo-Rosales, L. Campo-Deaño, Q. Huang, O. Hassager, and G. Petekidis, “Dilatancy in dense suspensions of model hard-sphere-like colloids under shear and extensional flow,” *J. Rheol.* **64**(5), 1179–1196 (2020).
- [19] Seto, R., and M. Doi, “Pressure-driven flow and jamming of dense suspensions in channels,” presented at the Virtual Symposium on the Physics of Dense Suspensions, July 9–10, 2020.
- [20] Baumgarten, A. S., and K. Kamrin, “Modeling stress relaxation in dense, fine-particle suspensions,” *J. Rheol.* **64**(2), 367–377 (2020).
- [21] Gillissen, J. J. J., C. Ness, J. D. Peterson, H. J. Wilson, and M. E. Cates, “Constitutive model for shear-thickening suspensions: Predictions for steady shear with superposed transverse oscillations,” *J. Rheol.* **64**(2), 353–365 (2020).
- [22] Dong, J., and M. Trulsson, “Unifying viscous and inertial regimes of discontinuous shear thickening suspensions,” *J. Rheol.* **64**(2), 255–266 (2020).
- [23] Madraki, Y., A. Oakley, A. Nguyen Le, G. Ovarlez, and S. Hormozi, “Shear thickening in dense non-Brownian suspensions: Viscous to inertial transition,” *J. Rheol.* **64**(2), 227–238 (2020).
- [24] Vasisht, V. V., M. Le Goff, K. Martens, and J. -L. Barrat, “Permanent shear localization in dense disordered materials due to microscopic inertia,” [arXiv:1812.03948](https://arxiv.org/abs/1812.03948) (2018).
- [25] Richards, J. A., B. M. Guy, E. Blanco, M. Hermes, G. Poy, and W. C. K. Poon, “The role of friction in the yielding of adhesive non-Brownian suspensions,” *J. Rheol.* **64**(2), 405–412 (2020).
- [26] Vo, T. T., S. Nezamabadi, P. Mutabaruka, J.-Y. Delenne, and F. Radjai, “Additive rheology of complex granular flows,” *Nat. Commun.* **11**(1), 1476 (2020).
- [27] Wang, G., A. M. Fiore, and J. W. Swan, “On the viscosity of adhesive hard sphere dispersions: Critical scaling and the role of rigid contacts,” *J. Rheol.* **63**(2), 229–245 (2019).
- [28] Seiphoori, A., X.-G. Ma, P. E. Arratia, and D. J. Jerolmack, “Formation of stable aggregates by fluid-assembled solid bridges,” *Proc. Natl. Acad. Sci. U. S. A.* **117**(7), 3375–3381 (2020).
- [29] Caggioni, M., V. Trappe, and P. T. Spicer, “Variations of the Herschel–Bulkley exponent reflecting contributions of the viscous continuous phase to the shear rate-dependent stress of soft glassy materials,” *J. Rheol.* **64**(2), 413–422 (2020).
- [30] Martys, N. S., W. L. George, R. P. Murphy, and K. M. Weigandt, “Pipe flow of sphere suspensions having a power-law-dependent fluid matrix,” *J. Rheol.* **64**(2), 445–457 (2020).
- [31] Bonnecaze, R. T., F. Khabaz, L. Mohan, and M. Cloitre, “Excess entropy scaling for soft particle glasses,” *J. Rheol.* **64**(2), 423–431 (2020).
- [32] Koumakis, N., J. F. Brady, and G. Petekidis, “Complex oscillatory yielding of model hard-sphere glasses,” *Phys. Rev. Lett.* **110**, 178301 (2013).
- [33] James, N. M., C.-P. Hsu, N. D. Spencer, H. M. Jaeger, and L. Isa, “Tuning interparticle hydrogen bonding in shear-jamming suspensions: Kinetic effects and consequences for tribology and rheology,” *J. Phys. Chem. Lett.* **10**(8), 1663–1668 (2019).
- [34] Hsu, C.-P., J. Mandal, S. N. Ramakrishna, N. D. Spencer, and L. Isa, “Exploring the roles of roughness, friction and adhesion in discontinuous shear thickening by means of thermo-responsive particles,” [arXiv:2004.05970](https://arxiv.org/abs/2004.05970)

- [35] Singh, A., R. Mari, M. M. Denn, and J. F. Morris, “A constitutive model for simple shear of dense frictional suspensions,” *J. Rheol.* **62**(2), 457–468 (2018).
- [36] Park, J. D., K. H. Ahn, and N. J. Wagner, “Structure-rheology relationship for a homogeneous colloidal gel under shear startup,” *J. Rheol.* **61**(1), 117–137 (2017).
- [37] Barthel, H., “Particle sizes of fumed silica,” *Chem. Eng. Technol.* **8**, 745–752 (1998).
- [38] Wyart, M., and M. E. Cates, “Discontinuous shear thickening without inertia in dense non-Brownian suspensions,” *Phys. Rev. Lett.* **112**, 098302 (2014).
- [39] Brown, E., N. A. Forman, C. S. Orellana, H. Zhang, B. W. Maynor, D. E. Betts, J. M. DeSimone, and H. M. Jaeger, “Generality of shear thickening in dense suspensions,” *Nat. Mater.* **9**, 220–224 (2010).
- [40] James, N., E. Han, J. Jureller, and H. Jaeger, “Interparticle hydrogen bonding can elicit shear jamming in dense suspensions,” *Nat. Mater.* **17**, 965–970 (2018).
- [41] Osuji, C. O., C. Kim, and D. A. Weitz, “Shear thickening and scaling of the elastic modulus in a fractal colloidal system with attractive interactions,” *Phys. Rev. E* **77**, 060402 (2008).
- [42] Lewis, T. B., and L. E. Nielsen, “Viscosity of dispersed and aggregated suspensions of spheres,” *Trans. Soc. Rheol.* **12**, 421 (1968).
- [43] Ness, C., and J. Sun, “Shear thickening regimes of dense non-Brownian suspensions,” *Soft Matter* **12**(3), 914–924 (2016).
- [44] Mari, R., R. Seto, J. F. Morris, and M. M. Denn, “Shear thickening, frictionless and frictional rheologies in non-Brownian suspensions,” *J. Rheol.* **58**(6), 1693–1724 (2014).
- [45] Mari, R., R. Seto, J. F. Morris, and M. M. Denn, “Discontinuous shear thickening in Brownian suspensions by dynamic simulation,” *Proc. Natl. Acad. Sci. U. S. A.* **112**(50), 15326–15330 (2015).
- [46] Ball, R., and J. R. Melrose, “A simulation technique for many spheres in quasi-static motion under frame-invariant pair drag and Brownian forces,” *Phys. A* **247**, 444–472 (1997).
- [47] Seto, R., R. Mari, J. F. Morris, and M. M. Denn, “Discontinuous shear thickening of frictional hard-sphere suspensions,” *Phys. Rev. Lett.* **111**(21), 218301 (2013).
- [48] Seto, R., G. G. Giusteri, and A. Martiniello, “Microstructure and thickening of dense suspensions under extensional and shear flows,” *J. Fluid Mech.* **825**, R3 (2017).
- [49] Cheal, O., and C. Ness, “Rheology of dense granular suspensions under extensional flow,” *J. Rheol.* **62**(2), 501–512.
- [50] More, R. V., and A. M. Ardekani, “Effect of roughness on the rheology of concentrated non-Brownian suspensions: A numerical study,” *J. Rheol.* **64**(1), 67–80 (2020).
- [51] Comtet, J., G. Chatté, A. Niguès, L. Bocquet, A. Siria, and A. Colin, “Pairwise frictional profile between particles determines discontinuous shear thickening transition in non-colloidal suspensions,” *Nat. Commun.* **8**, 1–7 (2017).
- [52] Brizmer, V., Y. Kligerman, and I. Etsion, “Elastic-plastic spherical contact under combined normal and tangential loading in full stick,” *Tribol. Lett.* **25**(1), 61–70 (2007).
- [53] Sedes, O., “Stress correlations and network analysis of shear thickening suspensions,” Ph.D. thesis (CUNY City College of New York, 2020).
- [54] Kulkarni, S. D., “Dense suspension rheology and flow phenomena,” Ph.D. thesis (City University of New York 2010).
- [55] Peyneau, P. E., and J. N. Roux, “Frictionless bead packs have macroscopic friction, but no dilatancy,” *Phys. Rev. E* **78**, 011307 (2008).
- [56] Thomas, J., K. Ramola, A. Singh, R. Mari, J. F. Morris, and B. Chakraborty, “Microscopic origin of frictional rheology in dense suspensions: Correlations in force space,” *Phys. Rev. Lett.* **121**, 128002 (2018).
- [57] Boyer, F., E. Guazzelli, and O. Pouliquen, “Unifying suspension and granular rheology,” *Phys. Rev. Lett.* **107**, 188301 (2011).
- [58] Nampoothiri, J. N., Y. Wang, K. Ramola, J. Zhang, S. Bhattacharjee, and B. Chakraborty, “Emergent elasticity in amorphous solids,” *Phys. Rev. Lett.* **125**, 118002 (2020).
- [59] Liu, T., F. Khabaz, R. T. Bonnecaze, and M. Cloitre, “On the universality of the flow properties of soft-particle glasses,” *Soft matter* **14**(34), 7064–7074 (2018).
- [60] Seth, J. R., L. Mohan, C. Locatelli-Champagne, M. Cloitre, and R. T. Bonnecaze, “A micromechanical model to predict the flow of soft particle glasses,” *Nat. Mater.* **10**(11), 838–843 (2011).
- [61] Liu, A., and S. Nagel, “Jamming is not just cool any more,” *Nature* **396**, 21 (1998).
- [62] Peters, I. R., S. Majumdar, and H. M. Jaeger, “Direct observation of dynamic shear jamming in dense suspensions,” *Nature* **532**, 214–217 (2016).
- [63] Mari, R., F. Krzakala, and J. Kurchan, “Jamming versus glass transitions,” *Phys. Rev. Lett.* **103**, 025701 (2009).
- [64] Pradeep, S., and L. C. Hsiao, “Contact criterion for suspensions of smooth and rough colloids,” *Soft Matter* **16**, 4980–4989 (2020).
- [65] Gameiro, M., A. Singh, L. Kondic, K. Mischaikow, and J. F. Morris, “Interaction network analysis in shear thickening suspensions,” *Phys. Rev. Fluids* **5**, 034307 (2020).
- [66] Pednekar, S., J. Chun, and J. F. Morris, “Bidisperse and polydisperse suspension rheology at large solid fraction,” *J. Rheol.* **62**, 513–526 (2018).
- [67] Barcelos, E. L., S. Khani, A. Boromand, L. F. Vieira, J. Alex Lee, J. Peet, M. F. Naccache, and J. Maia, “Controlling particle penetration and depletion at the wall using dissipative particle dynamics,” *Comput. Phys. Commun.* **258**, 107618 (2021).
- [68] Gauthier, A., M. Pruvost, O. Gamache, and A. Colin, “A new pressure sensor array for local normal stress measurement in complex fluids,” [arXiv:2010.04474](https://arxiv.org/abs/2010.04474)
- [69] Dbouk, T., L. Lobry, and E. Lemaire, “Normal stresses in concentrated non-Brownian suspensions,” *J. Fluid Mech.* **715**, 239–272 (2013).
- [70] Ovarlez, G., A. V. N. Le, W. J. Smit, A. Fall, R. Mari, G. Chatté, and A. Colin, “Density waves in shear-thickening suspensions,” *Sci. Adv.* **6**(16), eaay5589 (2020).
- [71] Lootens, D., H. Van Damme, Y. Hémar, and P. Hébraud, “Dilatant flow of concentrated suspensions of rough particles,” *Phys. Rev. Lett.* **95**, 268302 (2005).
- [72] Maranzano, B. J., and N. J. Wagner, “The effects of particle size on reversible shear thickening of concentrated colloidal dispersions,” *J. Chem. Phys.* **114**(23), 10514–10527 (2001).
- [73] Isa, L., R. Besseling, A. N. Morozov, and W. C. K. Poon, “Velocity oscillations in microfluidic flows of concentrated colloidal suspensions,” *Phys. Rev. Lett.* **102**, 058302 (2009).
- [74] Nott, P. R., and J. F. Brady, “Pressure-driven flow of suspensions: Simulation and theory,” *J. Fluid Mech.* **275**, 157–199 (1994).
- [75] Morris, J. F., and F. Boulay, “Curvilinear flows of noncolloidal suspensions: The role of normal stresses,” *J. Rheol.* **43**(5), 1213–1237 (1999).
- [76] Baumgarten, A. S., and K. Kamrin, “A general constitutive model for dense, fine-particle suspensions validated in many geometries,” *Proc. Natl. Acad. Sci. U. S. A.* **116**, 20828–20836 (2019).
- [77] Baumgarten, A. S., and K. Kamrin, “A general fluid–sediment mixture model and constitutive theory validated in many flow regimes,” *J. Fluid Mech.* **861**, 721–764 (2019).
- [78] Trulsson, M., B. Andreotti, and P. Claudin, “Transition from the viscous to inertial regime in dense suspensions” *Phys. Rev. Lett.* **109**, 118305 (2012).

- [79] Trulsson, M., E. de Giuli, and M. Wyart, "Effect of friction on dense suspension flows of hard particles," *Phys. Rev. E* **95**, 012605 (2017).
- [80] Richards, J.A., O'Neill, R.E., and Poon, W.C.K. "Turning a yield-stress calcite suspension into a shear-thickening one by tuning inter-particle friction," [arXiv:2007.05433](https://arxiv.org/abs/2007.05433) (2020).
- [81] Blanco, E., D. J. M. Hodgson, M. Hermes, R. Besseling, G. L. Hunter, P. M. Chaikin, M. E. Cates, I. Van Damme, and W. C. K. Poon, "Conching chocolate is a prototypical transition from frictionally jammed solid to flowable suspension with maximal solid content," *Proc. Natl. Acad. Sci. U. S. A.* **116**(21), 10303–10308 (2019).
- [82] Amarsid, L., J.-Y. Delenne, P. Mutabaruka, Y. Monerie, F. Perales, and F. Radjai, "Viscoinertial regime of immersed granular flows," *Phys. Rev. E* **96**, 012901 (2017).
- [83] Baranyai, A., and D. J. Evans, "On the entropy of the hard-sphere fluid," *J. Phys. Sci.* **46**, 27–31 (1991).
- [84] Larson, R. G., "The elastic stress in "film fluids"," *J. Rheol.* **41**, 365–372 (1997).